

Renormalization group analysis of phase transitions in the two dimensional Majorana-Hubbard model

by

Kyle Patrick Wamer

B.Sc., The University of Toronto, 2016

A THESIS SUBMITTED IN PARTIAL FULFILLMENT OF
THE REQUIREMENTS FOR THE DEGREE OF

MASTER OF SCIENCE

in

The Faculty of Graduate and Postdoctoral Studies

(Physics)

THE UNIVERSITY OF BRITISH COLUMBIA

(Vancouver)

August 2018

© Kyle Patrick Wamer 2018

Committee Page

The following individuals certify that they have read, and recommend to the Faculty of Graduate and Postdoctoral Studies for acceptance, the thesis entitled:

Renormalization group analysis of phase transitions in the two dimensional Majorana-Hubbard model

submitted by Kyle Patrick Wamer in partial fulfilment of the requirements for the degree of Master of Science in Physics.

Examining Committee:

Ian Affleck, Physics and Astronomy

Supervisor

Fei Zhou, Physics and Astronomy

Supervisory Committee Member

Abstract

A lattice of interacting Majorana modes can occur in a superconducting film on a topological insulator in a magnetic field. The phase diagram as a function of interaction strength for the square lattice was analyzed recently using a combination of mean field theory and renormalization group methods, and was found to include second order phase transitions. One of these corresponds to spontaneous breaking of an emergent $U(1)$ symmetry, for attractive interactions. Despite the fact that the $U(1)$ symmetry is not exact, this transition was claimed to be in a supersymmetric universality class when time reversal symmetry is present and in the conventional XY universality class otherwise. Another second order transition was predicted for repulsive interactions with time reversal symmetry to be in the same universality class as the transition occurring in the Gross-Neveu model, despite the fact that the $U(1)$ symmetry is not exact in the Majorana model. We analyze these phase transitions using a modified ϵ -expansion, confirming the previous conclusions.

Lay Summary

At zero degrees Celsius, water freezes. This is an example of a *phase transition* between two phase of the molecule H_2O : liquid water and ice. Phase transitions occur in all materials, and their classification has led to great discoveries across all branches of physics. Recently, a class of materials has been discovered with a unique feature: on their surfaces, these materials can exhibit a new type of particle, called a Majorana particle, that has been observed nowhere else in nature. In this thesis, we use a model of Majorana particles to predict the phase transitions that may occur on the surface of these novel materials. This research may have applications in the field of computer science, where scientists are attempting to use Majorana particles to create the first quantum computer – a machine that uses quantum mechanics to solve problems faster than a conventional computer.

Table of Contents

Abstract	iii
Lay Summary	iv
Table of Contents	v
List of Figures	vii
Acknowledgements	viii
Dedication	ix
1 Introduction	1
2 The Majorana-Hubbard Model	3
2.1 The Majorana-Hubbard Model on the Square Lattice	4
2.2 Low Energy Field Theory	6
2.2.1 Hubbard-Stratonovich Transformation	8
2.3 Symmetry Constraints on U(1) Breaking Operators	9
2.3.1 Quadratic Operators	10
2.3.2 Quartic Operators	10
2.3.3 Fermion-Boson Operators	11
3 Renormalization Group Methods	12
3.1 Beta Functions	12
3.2 Wilson's Approach to Renormalization	13
3.3 Dimensional Regularization	15
3.3.1 Modified Minimal Subtraction Scheme	16
3.4 The Epsilon Expansion	16
3.5 Modified Epsilon Expansion	18
3.5.1 Propagators	20
3.5.2 An Expansion in $d = 3 + (1 - \epsilon)$ Dimensions	21

Table of Contents

4 Renormalization of U(1) Breaking Operators	23
4.1 U(1) Breaking Operators with Attractive Interactions	24
4.1.1 Feynman Diagrams	24
4.1.2 Beta Functions of U(1) Breaking Operators	30
4.2 U(1) Breaking Operators with Repulsive Interactions	31
4.2.1 Feynman Diagrams	31
4.2.2 Beta Functions of U(1) Breaking Operator	32
5 Relevance of the Fermion Mass Operator	33
5.1 The Power of Supersymmetry	33
5.1.1 Superspace Formalism	34
5.1.2 Relating the fermion beta function and the stability critical exponent	35
5.2 Fermion Mass Beta Function	37
5.3 Consequence of a Relevant Fermion Mass Operator	38
6 Conclusion	40
Bibliography	41

Appendices

A Derivation of the Low Energy Field Theory	44
A.1 Quadratic Hamiltonian	44
A.2 Quartic Hamiltonian	45
A.3 Leading U(1) Breaking Operator	46
B Promoting ψ to a Dirac Fermion in Four Dimensions	48
C Two Loop Calculation of the Fermion Mass Beta Function	50
C.1 One Loop Diagrams	51
C.1.1 Fermion Propagator	51
C.1.2 Boson Propagator	53
C.1.3 Interaction Vertex	54
C.2 Two Loop Diagrams	54
C.2.1 Boson Counterterm Diagram	54
C.2.2 Fermion Counterterm Diagram	55
C.2.3 Internal Boson Bubble Diagram	56
C.2.4 Internal Fermion Bubble Diagram	58
C.2.5 Fermion Mass Beta Function	60

List of Figures

2.1	Proposed phase diagram of the Majorana-Hubbard model with time reversal symmetry	5
4.1	Fermion self energy diagram in Wilson RG for $g > 0$	25
4.2	Boson self energy diagram in Wilson RG	26
4.3	First diagram renormalizing h_3 and h_4 in Wilson RG.	27
4.4	Second diagram renormalizing h_3 and h_4 in Wilson RG	28
4.5	Fermion self energy in Wilson RG for $g < 0$	31
5.1	Diagram generating $\phi^4 + \text{h.c.}$ when the fermion mass is relevant	39
C.1	Fermion self energy in renormalized perturbation theory	51
C.2	Boson self energy in renormalized perturbation theory	53
C.3	Boson counterterm diagram in renormalized perturbation the- ory	55
C.4	Fermion counterterm diagram in renormalized perturbation theory	56
C.5	Two loop diagram with internal boson bubble in renormalized perturbation theory	57
C.6	Two loop diagram with internal fermion bubble in renormal- ized perturbation theory	58

Acknowledgements

I would like to thank my supervisor, Ian Affleck, for his support and mentorship during this project. I would also like to thank Joseph Maciejko and Igor Klebanov for helpful comments.

Dedication

To my mother, for her encouragement, enthusiasm and unwavering optimism that has made me never doubt what is possible.

To my father, for his tireless hard work that has given me the opportunity to pursue an education, and has inspired me to produce my best work.

To Gaby Hébert, for her loving support, and sense of adventure that has left me with so many great memories from these past two years.

Chapter 1

Introduction

In 1928, PAM Dirac proposed the existence of the positron: a particle with the same mass and spin as the electron, but with opposite charge [1]. The positron (and electron) are examples of Dirac fermions: particles which have distinct antiparticles of the same mass, but with opposite physical charges. Dirac fermions can be contrasted with fermions that equal their own antiparticle, known as Majorana fermions [2]. While the positron was detected shortly after Dirac's prediction [3], a Majorana particle has never been observed in particle physics.

In condensed matter physics, a Majorana fermion can arise despite the absence of fundamental Majorana particles, as an emergent phenomenon. Following the discovery of topological materials, it has been predicted that Majorana excitations appear in various situations at topological defects and boundaries of topological insulators [4, 5]. In fact, this prediction has led to an intense effort to develop a topological quantum computer that utilizes the physics of Majorana fermions [2, 4].

A setting in which a macroscopic number of interacting Majorana fermions is predicted to occur is a layer of ordinary superconductor on a strong topological insulator in a transverse magnetic field. The resulting vortex lattice is predicted to have a Majorana mode localized at every vortex core [2]. While there has been renewed interest in Majorana physics over the past decade, interaction effects have not been considered until recently. Much of the work on this subject has stemmed from the development of the Majorana-Hubbard model – a version of the Hubbard model involving Hermitian operators, and a four-site interaction term. [6–10]. This is the simplest interaction possible since a Hermitian Majorana operator obeying a canonical anticommutation relation will square to unity.

In this thesis, we study the critical behaviour of the Majorana-Hubbard model on the square lattice in two spatial dimensions. In Chapter 2, we introduce the model, discuss its features, and review the mean-field predictions made in [10]. We then review and extend the low energy field theory describing the predicted gapless phases of this model, for both repulsive and attractive interactions. A unique feature of this model is that it possesses an

emergent $U(1)$ symmetry, unlike the exact $U(1)$ that is assumed in related models [11–16]. One of the major tasks of this thesis is to determine the role that $U(1)$ breaking operators may have on the phase diagram. In Chapter 3, we introduce various renormalization group methods that will be used to study these operators. Then, in Chapter 4, we show that all $U(1)$ breaking operators are irrelevant to one loop order, using an ϵ -expansion and Wilson’s approach to the renormalization group. Finally, in Chapter 5, we consider the effects of a time reversal breaking perturbation, a fermion mass term, on the Majorana-Hubbard model. Using a combination of renormalization group and supersymmetry methods, we show that such a perturbation is relevant, and results in a critical point in the conventional XY universality class. If time reversal is an approximate symmetry, the critical point may exhibit signs of $\mathcal{N} = 2$ supersymmetry, which has previously been realized in [11–15]. Just like the Majorana particle, supersymmetry is a prediction from high energy theory that has not yet been verified experimentally. Based on our results, we propose that the Majorana-Hubbard model on a square lattice is a candidate system for realizing the signatures of supersymmetry in an experimentally realizable set-up.

Chapter 2

The Majorana-Hubbard Model

In the theory of topological materials, a Majorana mode is predicted to occur at the core of a vortex on the surface of a superconducting layer placed on a strong topological insulator [2]. A lattice of vortices will occur when this layered material is placed in a transverse magnetic field, and it is believed that the corresponding Majorana lattice will exhibit interactions that fall off exponentially with the superconducting coherence length [9]. We denote by γ_j the Majorana fermion operator at lattice site j . Since these operators are Hermitian, the canonical anticommutation relation

$$\{\gamma_i, \gamma_j\} = 2\delta_{ij} \quad (2.1)$$

implies that the shortest possible range interaction term must occur on 4 sites (an odd number of sites would lead to a Hamiltonian that is not a bosonic operator). The simplest model describing a lattice of interacting Majorana fermions is then the Majorana-Hubbard model – a Hamiltonian with nearest neighbour hopping and shortest possible range 4-site interaction term:

$$H = it \sum_{\langle ij \rangle} e^{i\phi_{ij}} \gamma_i \gamma_j + g \sum_{[ijkl]} \gamma_i \gamma_j \gamma_k \gamma_l \quad (2.2)$$

Here $\langle ij \rangle$ denotes nearest neighbour lattice sites, and $[ijkl]$ denotes sets of 4 closest lattice sites. The phase factor $e^{i\phi_{ij}}$ is determined by the requirement that one superconducting flux quantum passes through each lattice point, giving rise to one Majorana fermion at each site [9, 17]. This model was first introduced by Stern and Grosfeld in the context of the fractional quantum Hall effect [17].

In one dimension, the Majorana-Hubbard model was shown to have an interesting phase diagram [6–8]. At large enough interaction strength g , the Majorana modes on the chain dimerize to form (non-Hermitian) Dirac fermions, breaking translational symmetry. In the case of $g > 0$, this phase transition was shown to be described by the tricritical Ising model, which

exhibits supersymmetry. As we will see below, this manifestation of supersymmetry is not unique to one dimension.

More recently, the Majorana-Hubbard model has been studied in two dimensions on the square lattice [10, 18] and the honeycomb lattice [19]. In this thesis, we restrict our attention to the square lattice in two dimensions.

2.1 The Majorana-Hubbard Model on the Square Lattice

On the square lattice, the interaction term occurs on plaquettes:

$$H = it \sum_{m,n} \gamma_{m,n} [(-1)^n \gamma_{m+1,n} + \gamma_{m,n+1}] + g \sum_{m,n} \gamma_{m,n} \gamma_{m+1,n} \gamma_{m+1,n+1} \gamma_{m,n+1} \quad (2.3)$$

The phase factor $e^{i\phi_{ij}}$ in (2.2) has been fixed so that there is π magnetic flux through each plaquette, corresponding to one vortex at each site, according to [9, 17]. The sign of t can be changed by a \mathbb{Z}_2 gauge transformation

$$\gamma_{m,n} \rightarrow s_{m,n} \gamma_{m,n} \quad s_{m,n} = \pm 1 \quad (2.4)$$

but cannot be completely removed [10]. Without loss of generality, we assume $t > 0$. When $g > 0$, the underlying physical interactions are attractive, as can be shown using mean field theory, or by mapping the theory to its continuum limit (see below).

This model was studied in detail in [10], where it was shown to have a rich phase diagram as a function of gt^{-1} (Figure 2.1). The large g limit was also studied recently in [18]. As in the one dimensional Majorana-Hubbard model, at strong enough coupling, the Majorana modes like to pair up on neighbouring sites to form Dirac fermions, breaking translation symmetry in either the horizontal or vertical direction. For $g > 0$, the Dirac fermions' energy levels are empty, while they alternate being empty and occupied for $g < 0$. We call these dimerized phases 'ferromagnetic' (FM) and 'antiferromagnetic' (AFM), respectively. Furthermore, two second order phase transitions were predicted to occur at $g = g_{c,1} \approx -0.9t$ and $g = g_{c,2} \approx +0.9t$. The dotted line in Figure 2.1 is a first order phase transition that does not have an interpretation in terms of Majorana pairings.

By deriving the low energy continuum limit of (2.3), emergent Lorentz and U(1) symmetries were found to occur at these transitions. In terms of a 2-component complex fermion ψ , the imaginary time Lagrangian density was found to be

$$\mathcal{L}_{U(1)} = \bar{\psi} \gamma^\mu \partial_\mu \psi + 64g\Lambda_0^{-2} (\bar{\psi}\psi)^2. \quad (2.5)$$

2.1. The Majorana-Hubbard Model on the Square Lattice

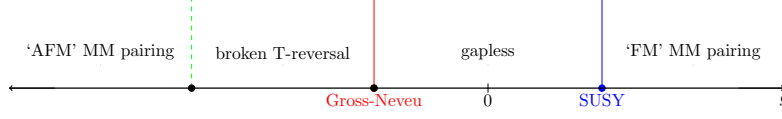


Figure 2.1: Proposed phase diagram of the Majorana-Hubbard model with time reversal symmetry

Here $\bar{\psi} := \psi^\dagger \gamma^0$, and the Dirac gamma matrices, γ^μ , satisfy

$$\gamma^\mu := \{\sigma_y, \sigma_x, -\sigma_z\} \quad \{\gamma^\mu, \gamma^\nu\}_{ab} = 2\delta_{ab}. \quad (2.6)$$

The coefficient $\Lambda_0 = a^{-1}$ is a bare cutoff defined by the inverse lattice spacing, a , and the imaginary time coordinate has been rescaled so that the velocity $v = 4ta \equiv 1$. Using (2.5), it was argued that the phase transition at $g_{c,1}$ is in the universality class of the Gross-Neveu model, while the transition at $g_{c,2}$ corresponds to the $\mathcal{N} = 2$ supersymmetric (SUSY) universality class.

When a fermion mass term $\bar{\psi}\psi$ is present, it was further argued that supersymmetry is broken, and the transition at $g_{c,2}$ falls into the XY universality class (the $g_{c,1}$ transition is not present in the massive case). Such a term can be generated by adding a second-neighbour hopping to the Hamiltonian:

$$H \rightarrow H + it_2 \sum_{m,n} \sum_{s,s'=\pm 1} \gamma_{m,2n} \gamma_{m+s,2n+s'} \quad (2.7)$$

This term breaks time reversal symmetry (see (2.28)) and should be included in any model hoping to describe a vortex lattice in a transverse magnetic field.

In this thesis, we use renormalization group methods to check the universality class predictions for $g_{c,1}$ and $g_{c,2}$ made in [10]. In particular, we will use an ϵ -expansion to determine the relevance of leading $U(1)$ breaking operators and the fermion mass term. In the next section, we begin by re-deriving the low energy field theory and calculating the leading $U(1)$ breaking corrections. We then introduce a boson (real or complex, depending on the sign of g), using a Hubbard-Stratonovich transformation. These fermion-boson models will be the starting point of our renormalization group analysis in later chapters.

2.2 Low Energy Field Theory

Due to the alternating nature of the nearest neighbour hopping in (2.3), the unit cell spans two lattice sites, so we define

$$\gamma_{m,2n} = \gamma_{m,2n}^e \quad \gamma_{m,2m+1} = \gamma_{m,2n+1}^o. \quad (2.8)$$

These definitions of $\gamma^{e/o}$ are slightly different than those of [10], and are chosen to simplify the form of the U(1) breaking operators. To derive a low energy field theory, we start with the dispersion relation of the non-interacting model ($g = 0$):

$$E_{\pm} = \pm 4t \sqrt{\sin^2 k_x + \sin^2 k_y}. \quad (2.9)$$

We then replace each Majorana operator $\gamma^{e/o}$ with a combination of two slowly varying Majorana fields $\chi^{e/o,\pm}$, according to

$$\gamma^{e/o}(\vec{r}) \approx 2\sqrt{2}\Lambda_0^{-1}[\chi^{e/o+}(\vec{r}) + (-1)^x \chi^{e/o-}(\vec{r})]. \quad (2.10)$$

These fields χ^{\pm} consist of the momenta modes of γ near the two Dirac points of the non-interacting theory, which occur at $\vec{k} = (0,0)$ and $\vec{k} = (\pi/a,0)$. The coefficient $\Lambda_0^{-1} = a$ is the lattice spacing, and its inverse defines a bare energy cutoff of the theory. To derive the continuum limit, we Taylor expand the quadratic and quartic pieces of (2.3) in Appendix A. We expand the quartic operator to two derivatives, while keeping only leading order quadratic terms, since the underlying symmetry of the lattice model forbids any quadratic operator from breaking the U(1) symmetry (as proven below). The resulting Hamiltonian density is

$$\mathcal{H} = 4ita \sum_{\pm} \left[\pm \chi^{e\pm} \partial_x \chi^{e\pm} \mp \chi^{o\pm} \partial_x \chi^{o\pm} + 2\chi^{e\pm} \partial_y \chi^{o\pm} \right] + \mathcal{H}_{\text{int}} \quad (2.11)$$

where

$$\begin{aligned} \frac{1}{64g\Lambda_0^{-4}} \mathcal{H}_{\text{int}} = & -4\Lambda_0^2 \chi^{e-} \chi^{e+} \chi^{o-} \chi^{o+} - \sum_{s,s'=\pm} ss' \chi^{es} \partial_x \chi^{es} \chi^{os'} \partial_x \chi^{os'} + 2\partial_y (\chi^{e-} \chi^{e+}) \partial_y (\chi^{o-} \chi^{o+}) \\ & + 2\chi^{e-} \chi^{e+} \partial_x \chi^{o-} \partial_x \chi^{o+} + 2\partial_x \chi^{e-} \partial_x \chi^{e+} \chi^{o-} \chi^{o+} + \partial_x (\chi^{e-} \chi^{e+}) \partial_x (\chi^{o-} \chi^{o+}). \end{aligned} \quad (2.12)$$

We introduce two-component Majorana fermions $\chi^+ := (\chi^{e+}, \chi^{o+})^T$ and $\chi^- := (\chi^{o-}, \chi^{e-})^T$, so that the first term of (2.11) becomes

$$\mathcal{H}_0 := \mathcal{H} - \mathcal{H}_{\text{int}} = 4ita \sum_{\pm} \chi^{\pm T} [\sigma^z \partial_x + \sigma^x \partial_y] \chi^{\pm}. \quad (2.13)$$

2.2. Low Energy Field Theory

These two-component Majorana fermions satisfy the canonical anti-commutation relations $\{\chi^i(\vec{r}), \chi^j(\vec{r}')\} = \delta^{ij}\delta(\vec{r} - \vec{r}')$. Since \mathcal{H}_{int} is not a function of $\partial_t \chi^\pm$, we have $\mathcal{L}_{\text{int}} = \mathcal{H}_{\text{int}}$ in imaginary time, and the Lagrangian density corresponding to (2.11) is

$$\mathcal{L} = \sum_{\pm} \bar{\chi}^\pm \gamma^\mu \partial_\mu \chi^\pm + \mathcal{H}_{\text{int}}. \quad (2.14)$$

We've set the velocity $v = 4ta$ to unity, used the Euclidean gamma matrices defined in (2.6), and defined $\bar{\chi}^\pm := \chi^{\pm T} \gamma^0$. In order to identify any emergent U(1) invariance of (2.14), we define a complex fermion ψ according to

$$\psi = \chi^+ + i\chi^- = \begin{pmatrix} \chi^{e+} + i\chi^{o-} \\ \chi^{o+} + i\chi^{e-} \end{pmatrix}. \quad (2.15)$$

In this language, the most relevant U(1) breaking operator in (2.14) is

$$16g\Lambda_0^{-4} \left(\psi_1 \psi_2 [\partial_x \psi_1 \partial_x \psi_2 - \partial_y \psi_1 \partial_y \psi_2] + \text{h.c.} \right) \quad (2.16)$$

as shown in Appendix A. Including this term, the low energy field theory describing (2.3) is

$$\mathcal{L} = \bar{\psi} \gamma^\mu \partial_\mu \psi + M \bar{\psi} \psi + 64g\Lambda_0^{-2} (\bar{\psi} \psi)^2 + 16g\Lambda_0^{-4} \left(\psi_1 \psi_2 \partial_r \psi_1 \partial_r \psi_2 + \text{h.c.} \right) \quad (2.17)$$

where we've introduced the notation

$$\partial_r \psi_a \partial_r \psi_b := \partial_x \psi_a \partial_x \psi_b - \partial_y \psi_a \partial_y \psi_b. \quad (2.18)$$

and we've also introduced a fermion mass term: As shown in [10], when the second-neighbour hopping term is included (see (2.7)),

$$\mathcal{L} \rightarrow \mathcal{L} + M \bar{\psi} \psi \quad M := 8t_2 \quad (2.19)$$

Since

$$(\bar{\psi} \psi)^2 = -\psi_1^* \psi_2^* \psi_2 \psi_1 \quad (2.20)$$

we see from (2.17) that $g > 0$ corresponds to underlying physical interactions that are attractive. As a last comment, we note that the Nielson Ninomiya theorem [20] is not violated here, even though we have achieved a single Dirac fermion on the lattice, since the U(1) symmetry is only emergent, and not exact.

2.2.1 Hubbard-Stratonovich Transformation

In the absence of the U(1) breaking operator, the interaction term in (2.17) is proportional to $(\bar{\psi}\psi)^2$. In this case, we expect a massless boson to appear at the phase transitions $g_{c,1}, g_{c,2}$, whose expectation value provides the order parameter of the transition [10, 16]. Such a boson can be introduced using a Hubbard-Stratonovich transformation. This procedure depends on the sign of the $(\bar{\psi}\psi)^2$ interaction: in the case of attractive interactions ($g > 0$), a complex charge-2 boson is introduced, while in the case of repulsive interactions ($g < 0$), a real boson is introduced. To promote these bosonic variables to dynamical fields, we reduce the energy scale of the continuum theory from Λ_0 down to some reduced scale $\Lambda \ll \Lambda_0$. Using the same symbols to denote these renormalized fields, we arrive at the following two imaginary time Lagrangian densities, depending on the sign of g :

- Repulsive Interactions ($g < 0$):

$$\mathcal{L}_1 = \bar{\psi}\gamma^\mu\partial_\mu\psi + (\partial_\mu\sigma)^2 + r^2\sigma^2 + \eta_1\sigma\bar{\psi}\psi + \eta_2^2\sigma^4 + h_1[\psi_1\psi_2\partial_r\psi_1\partial_r\psi_2 + \text{h.c.}] \quad (2.21)$$

- Attractive Interactions ($g > 0$):

$$\mathcal{L}_2 = \bar{\psi}\gamma^\mu\partial_\mu\psi + M\bar{\psi}\psi + |\partial_\mu\phi|^2 + m^2|\phi|^2 + \lambda_1[\phi^*\psi^TC\psi + \text{h.c.}] + \lambda_2^2|\phi|^4 + \mathcal{L}'_2 \quad (2.22)$$

where $C = i\gamma^0$ and

$$\mathcal{L}'_2 := h_2\psi_1\psi_2\partial_r\psi_1\partial_r\psi_2 + h_3\phi\partial_r\psi_1\partial_r\psi_2 + h_4\phi[\partial_r^2\psi_1\psi_2 + \psi_1\partial_r^2\psi_2] + \text{h.c.} \quad (2.23)$$

We have only included a fermion mass in the case of attractive interactions; the phase transition for $g < 0$ vanishes as soon as time reversal symmetry is broken, according to mean field theory [10]. Note that in the case of attractive interactions, two additional U(1) breaking operators are generated during this renormalization procedure. Such terms do not occur for a real boson σ , since they violate an underlying $\frac{\pi}{2}$ -rotation symmetry of the lattice, as explained in Section 2.3. The Greek coupling constants $\{\lambda_i, \eta_i\}$ precede U(1) preserving operators, while the Latin coupling constants $\{h_i\}$ precede U(1) breaking operators. Equations (2.21) and (2.22) will be the starting point for all of our calculations that follow. We will assume that the symmetry breaking parameters $\{h_i\}$ and M are small, so that the theories are close to their quantum critical points. This is not an unreasonable assumption for the lattice model: the U(1) breaking operators are superficially irrelevant,

2.3. Symmetry Constraints on $U(1)$ Breaking Operators

and are preceded by a factor of Λ_0^{-4} . At a reduced cutoff $\Lambda \ll \Lambda_0$, the coupling constants will be suppressed by four factors of Λ/Λ_0 . Of course, this argument is incomplete, as it ignores higher order renormalization effects. If the $\{h_i\}$ and M are not small, their flow will depend on the the presence of additional fixed points in parameter space.

We have assumed that under this renormalization, the velocities of the boson and fermion flow to a common value. This has been shown to be the case in the $U(1)$ invariant version of these models, and to linear order in M and $\{h_i\}$, we expect the same result to hold [12, 13]. The irrelevance of Lorentz breaking operators has also been established for fermion-boson models on the honeycomb lattice.[21–23] The fermion and boson velocities would be identical if Lorentz invariance was exact.

In [10], the nature of the transitions at $g_{c,1}$ and $g_{c,2}$ was predicted using the $U(1)$ symmetric versions of (2.21) and (2.22), and invoking universality. In the fermion-boson models, the transitions are driven by reducing the squared boson mass, and letting it change sign. The $U(1)$ symmetric version of (2.21) was considered in [16], and the transition was shown to correspond to that of the Gross-Neveu model, with spontaneous breaking of the \mathbb{Z}_2 symmetry

$$\sigma \rightarrow -\sigma \quad \bar{\psi}\psi \rightarrow -\bar{\psi}\psi \quad (2.24)$$

It is not the Ising transition, because an additional massless fermion field ψ is present. The $U(1)$ version of (2.22) involving the charge-2 boson ϕ , (2.22), has been studied as well [11–13, 15, 16], and the transition is known to exhibit $\mathcal{N} = 2$ supersymmetry when $M = 0$. This should not be confused with the $\mathcal{N} = 1$ supersymmetry that is present in [24].

2.3 Symmetry Constraints on $U(1)$ Breaking Operators

To complete this chapter, we comment on the symmetries of (2.17). The authors of [10] identified various exact symmetries of the lattice Hamiltonian (2.3), which must be obeyed at the continuum level. We label them C for charge conjugation, P for parity, and R for $\frac{\pi}{2}$ -spatial rotation. Explicitly, they are:

$$C : \quad \psi(x, y) \mapsto \psi^*(x, y) \quad (2.25)$$

$$P : \quad \psi(x, y) \mapsto -i\gamma^1 \psi^*(-x, y) \quad (2.26)$$

$$R : \quad \psi(x, y) \mapsto e^{-\frac{i\pi}{4}} e^{\frac{i\pi}{4}\gamma^0} \psi(-y, x) \quad (2.27)$$

2.3. Symmetry Constraints on $U(1)$ Breaking Operators

Additionally, in the special case of $t_2 = M = 0$, the model is also invariant under time reversal, T :

$$T : \psi(x, y) \mapsto -\gamma^0 \psi^*(x, y), \quad i \mapsto -i \quad (2.28)$$

In the following, we demonstrate how C and R are sufficient to ensure that all quadratic operators in the continuum theory preserve the $U(1)$ symmetry, as is in the case in (2.11). We then demonstrate how the $U(1)$ breaking term in (2.16) is the only possible quartic operator, with two or less derivatives, that satisfies the symmetries C, P and R . These results apply even when the fermion mass is nonzero, since neither argument requires the use of T . Finally, we explain how R limits the $U(1)$ breaking fermion-boson interactions to the ones present in (2.21) and (2.22).

2.3.1 Quadratic Operators

The most general $U(1)$ breaking quadratic operator (with or without derivatives) is of the form

$$\psi^T A \psi + \psi^\dagger A^\dagger \psi^* \quad (2.29)$$

for some differential operator $A(x, y)$. Under C ,

$$C : \psi^T A \psi + \psi^\dagger A^\dagger \psi^* \mapsto \psi^T A^\dagger \psi + \psi^\dagger A \psi^* \quad (2.30)$$

which forces A to be Hermitian. Under R ,

$$R : \psi^T A(x, y) \psi \mapsto -\frac{i}{2} \psi^T (1 - i\sigma_y) A(-y, x) (1 + i\sigma_y) \psi. \quad (2.31)$$

The right hand side of (2.31) cannot appear for nonzero A , since it is anti-Hermitian, and violates (2.30). Therefore, no charge 2 operator is allowed by symmetry.

2.3.2 Quartic Operators

One-Derivative Quartic Operators

A four-Fermi operator involving a single derivative can only have charge 0 or ± 2 : terms with charge ± 4 include at least three fermi fields without derivatives, and vanish by Fermi statistics. Since R is a combination of spatial rotation by $\frac{\pi}{2}$ and $U(1)$ rotation by $-\frac{\pi}{4}$, these two possibilities require, respectively, a derivative operator that transforms trivially or one that transforms with a prefactor of i . Of these, only the latter exists:

$$\partial_x + i\partial_y \quad (2.32)$$

but such an operator breaks CP .

Two-Derivative Quartic Operators

Repeating the previous argument, the derivative operator of a charge 2 four-fermi term must transform with a factor of i to satisfy R symmetry. This is not possible for a generic two-derivative operator $A_{ab}\partial_a\partial_b$, ruling out charge 2 operators. Charge 4 terms require a derivative operator that transforms with a prefactor of -1 to be invariant under R . By Fermi statistics, the two derivatives must act on separate Fermi fields, so the most general operators are

$$\psi_1\psi_2[\partial_x\psi_1\partial_x\psi_2 - \partial_y\psi_1\partial_y\psi_2] \quad (2.33)$$

and

$$\psi_1\psi_2[\partial_x\psi_1\partial_y\psi_2 - \partial_y\psi_1\partial_x\psi_2] \quad (2.34)$$

Of these, only the former is allowed, since the latter breaks CP . Therefore, the $U(1)$ breaking operator appearing in (2.14) is the only possible term with two or less derivatives.

2.3.3 Fermion-Boson Operators

In the case of attractive interactions, a complex boson $\phi \sim \psi_1\psi_2$ is introduced. Using (2.27), we see that

$$R : \phi(x, y) \rightarrow i\phi(-y, x) \quad (2.35)$$

Since $\psi^T C \psi$ also picks up a factor of i under R , the following two derivative, $U(1)$ breaking operators are invariant under R -symmetry:

$$\phi[\partial_x\psi_1\partial_x\psi_2 - \partial_y\psi_1\partial_y\psi_2] + \text{h.c.} \quad (2.36)$$

and

$$\phi[(\partial_x^2 - \partial_y^2)\psi_1\psi_2 + \psi_1(\partial_x^2 - \partial_y^2)\psi_2] + \text{h.c.} \quad (2.37)$$

It is easy to check that the remaining symmetries (2.25 - 2.27) also leave these operators invariant.

In the case of repulsive interactions, a real boson $\sigma \sim \bar{\psi}\psi$ is introduced, which is invariant under R :

$$R : \sigma(x, y) \rightarrow \sigma(-y, x) \quad (2.38)$$

Using the above constraints on pure fermion operators, the most relevant $U(1)$ breaking fermion-boson operator is then

$$\sigma^2\psi_1\psi_2[\partial_x\psi_1\partial_x\psi_2 - \partial_y\psi_1\partial_y\psi_2] \quad (2.39)$$

which is too irrelevant for our considerations.

Chapter 3

Renormalization Group Methods

In the previous chapter, we derived the low energy field theories that characterize the Majorana-Hubbard model near its quantum critical points $g_{c,1}$ and $g_{c,2}$ (equations (2.21) and (2.22)). Both of these theories contain operators that *a priori* do not let us easily determine their universality classes. The main result of this thesis will be to use the renormalization group to characterize these problematic operators, and determine the role they play near these two critical points. In this chapter, we review various methods from renormalization group theory that we will apply throughout the following chapters. This material is explained very clearly in the texts [25, 26], and in the paper [27].

3.1 Beta Functions

The fundamental idea behind the renormalization group is to quantify how the coupling constants of a theory depend on the choice of length scale. If a certain coupling constant increases as we increase the scale, we say the corresponding operator is *relevant*. If a coupling constant decreases at larger length scales, we say the corresponding operator is *irrelevant*. Finally, an operator whose coupling constant does not evolve is called *marginal*. In condensed matter theory, where there is often a great difference of scales between the ‘bare’ scale of the lattice constant and the observable scale of macroscopic phenomena, an irrelevant operator can safely be excluded from the effective Lagrangian. Thus, our task will be to show whether or not the U(1) breaking and T -breaking operators of (2.21) and (2.22) are irrelevant or not. If so, the classification of the related U(1) and T symmetric models of [10] may be applied here.

The equations describing the evolution of coupling constants as a function of length scale are known as beta functions. Given a family of length scales $b^{-1}\Lambda$, parametrized by $b = e^{\delta l}$, the beta function of coupling constant

3.2. Wilson's Approach to Renormalization

X is defined to be

$$\beta_X := \frac{dX}{d \log b} = \frac{dX}{d \delta l} \quad (3.1)$$

Relevant operators have positive beta functions, while irrelevant operators have negative ones. In some applications, such as those introduced in Section 3.3, it is more natural to quantify how coupling constants depend on a energy scale parameter μ , instead of a length scale. In this case,

$$\beta_X = -\frac{dX}{d \log \mu} \quad (3.2)$$

Beta functions can also be used to identify critical points. At a critical point, the system exhibits scale invariance, and the coupling constants do not evolve. In other words, critical point correspond to ‘fixed-points’ in parameter space, which are precisely the zeros of the beta functions.

We will calculate these beta functions using two different approaches to the renormalization group: 1) the Wilson, or ‘momentum shell’, approach, and 2) dimensional regularization.

3.2 Wilson's Approach to Renormalization

Much of our modern understanding of the renormalization group is thanks to Ken Wilson [28]. In his approach, one calculates beta functions by slightly reducing the energy scale of the theory by integrating out fields whose momentum modes lie in a thin shell in momentum space. This shell consists of all momenta with magnitude lying within $\{b^{-1}\Lambda, \Lambda\}$, where Λ is the UV cutoff of the original theory.

We will explain how this integration is carried out for the case of a single scalar field φ . This will introduce the notation that we will use in the following chapters for the more complicated field theories (2.21) and (2.22). The Lagrangian density is taken to be

$$\mathcal{L}_\varphi = \frac{1}{2}(\partial\varphi)^2 + \sum_i X_i \mathcal{O}_i[\varphi] \quad (3.3)$$

where $\mathcal{O}_i[\varphi]$ is a generic operator involving the field φ and its derivatives. We begin by separating the field into a slow and fast component

$$\varphi = \varphi_s + \varphi_f, \quad (3.4)$$

where φ_s contains the momentum modes of φ with magnitude less than $b^{-1}\Lambda$, and φ_f contains the modes that lie within the shell. In terms of these

3.2. Wilson's Approach to Renormalization

new variables, the Lagrangian density can be reorganized as follows:

$$\mathcal{L}_\varphi = \mathcal{L}_s + \mathcal{L}_f^0 + \mathcal{L}_{sf}. \quad (3.5)$$

The first term, \mathcal{L}_s , equals the original Lagrangian density, but with φ replaced with φ_s . The second term, \mathcal{L}_f^0 , equals the free fast Lagrangian density, $\frac{1}{2}(\partial\varphi_f)^2$. The remaining term contains all operators that mix slow and fast components. The partition function can then be rewritten as

$$Z = \int \mathcal{D}\varphi_s \varphi_f e^{-\int d^d x (\mathcal{L}_s + \mathcal{L}_f^0 + \mathcal{L}_{sf})} \quad (3.6)$$

$$= Z_{0,f} \int \mathcal{D}\varphi_s e^{-\int d^d x (\mathcal{L}_s + \delta\mathcal{L})} \quad (3.7)$$

where

$$Z_{0,f} := \int \mathcal{D}\varphi_f e^{-\int d^d x \mathcal{L}_f} \quad \langle \cdots \rangle_f := Z_{0,f}^{-1} \int \mathcal{D}\varphi_f \cdots e^{-\int d^d x \mathcal{L}_f} \quad (3.8)$$

and

$$e^{-\int d^d x \delta\mathcal{L}} := \langle e^{-\int d^d x \mathcal{L}_{sf}} \rangle_f \quad (3.9)$$

In other words, integrating out the fast modes has generated new terms in the Lagrangian. Since the operators appearing in (3.3) were generic, we can write

$$\delta\mathcal{L} = \frac{1}{2}\delta Z_\varphi (\partial\varphi_s)^2 + \sum_i \delta Z_i \mathcal{O}_i[\varphi_s] \quad (3.10)$$

in terms of *renormalization constants* δZ_φ and δZ_i . To compare $\mathcal{L}_s + \delta\mathcal{L}$ to the original theory, we rescale coordinates

$$x \rightarrow b^{-1}x \quad (3.11)$$

so that the new UV cutoff is once again Λ , and rescale the field

$$\varphi_s \rightarrow \varphi_s \sqrt{(1 + \delta Z_\varphi) b^{d-2}} \quad (3.12)$$

so that the new kinetic term is once again $\frac{1}{2}(\partial\varphi)^2$. Defining d_i and n_i to be the mass dimension and number of factors of φ , respectively, of \mathcal{O}_i , we find that the coupling constants of the reduced theory, $\{X_i(b)\}$, satisfy

$$X_i(b) = X_i \left(1 + \frac{\delta Z_i}{X_i} \right) (1 + \delta Z_\varphi)^{-n_i} b^{d_i} \quad (3.13)$$

3.3. Dimensional Regularization

This expression can now be differentiated with respect to $\log b$, yielding the beta functions of the theory, $\{\beta_{X_i}\}$.

While very physical, the Wilsonian approach to the renormalization group leads to complications beyond first order in perturbation theory, when nested momentum shell integrations are required. We now introduce a second approach to the renormalization group that is more suited for higher order calculations [25, 27].

3.3 Dimensional Regularization

Instead of explicitly changing the length scale of the theory, beta functions can also be calculated using a properly regularized theory at a fixed energy scale. Consider the following example Lagrangian density of a real scalar field:

$$\mathcal{L}_{\varphi^4} = \frac{1}{2}(\partial\varphi)^2 + m^2\varphi^2 + X\varphi^4 \quad (3.14)$$

This theory is not regularized: a perturbative expansion of its correlation functions will lead to divergences, order by order. To resolve this, we use a procedure known as dimensional regularization, in which we continue the spacetime dimension away from an integer, rendering momentum loop integrals finite. We then subtract off these contributions by introducing *counterterms* into the Lagrangian density, before continuing back to an integer dimension. This is performed at a given energy scale μ , which we fix.

For example, at one loop, the φ self energy receives a contribution proportional to

$$\int \frac{d^d p}{(2\pi)^d} \frac{1}{(p^2 + m^2)} \propto \Gamma\left(1 - \frac{d}{2}\right) \quad (3.15)$$

where $\Gamma(x)$ is the gamma function with poles at non-positive integers. For non-integer d , this expression is finite, and can be cancelled by introducing a counterterm

$$\delta Z_\varphi \frac{1}{2}(\partial\varphi)^2 \quad (3.16)$$

into the Lagrangian, with

$$\delta Z_\varphi \propto -\Gamma\left(1 - \frac{d}{2}\right) \quad (3.17)$$

Repeating these steps for all divergences at a given order, we arrive at a *renormalized Lagrangian* density at scale μ ,

$$\mathcal{L}_{\varphi^4,r} = \frac{1}{2}Z_\varphi(\partial\varphi_r)^2 + Z_m\mu^2 m_r^2\varphi_r^2 + Z_X\mu^{4-d}X_r\varphi_r^4, \quad (3.18)$$

3.4. The Epsilon Expansion

in terms of renormalized field φ_r and renormalized coupling constants m_r and X_r . The *renormalization constants* Z_i contain the introduced counterterms δZ_i according to

$$Z_i = 1 + \delta Z_i \quad (3.19)$$

The explicit energy scale μ enters to make the renormalized coupling constants dimensionless. Now, to extract the beta functions, we must relate the two Lagrangian densities (3.14) and (3.18). Matching kinetic terms, we find

$$\varphi = \sqrt{Z_\varphi} \varphi_r \quad (3.20)$$

and then rescaling, we find

$$m_r = m \mu^{-1} Z_\varphi Z_m^{-1} \quad (3.21)$$

$$X_r = X \mu^{4-d} Z_\varphi^2 Z_X^{-1} \quad (3.22)$$

These equations are the dimensional regularized analogues of (3.13). Differentiating with respect to $-\log \mu$ generates the desired beta functions.

3.3.1 Modified Minimal Subtraction Scheme

Exactly how the counterterms in (3.19) are defined leads to further choice in renormalization scheme. If only the divergent parts of the loop diagram are included in the counterterm, the scheme is known as ‘minimal subtraction’. In our calculations, we use the more common ‘modified minimal subtraction’ scheme, or \overline{MS} , which adds to the counterterm the universal constant $\log(e^{\gamma_E}/4\pi)$ that always occurs in Feynman diagrams. This is implemented by rescaling the energy scale $\mu \rightarrow \mu \frac{e^{\gamma_E}}{4\pi}$ in (3.18) [25, 27].

3.4 The Epsilon Expansion

In both the Wilsonian and dimensional regularization pictures of the renormalization group, we are tasked with calculating beta functions and determining their fixed points. In practice, these fixed points are often not accessible in two space dimensions and one time dimension; instead, one must consider the theory close to its upper critical dimension (UCD), and expand about this point. This procedure is known as the ϵ -expansion, and was first introduced to study the theory \mathcal{L}_{φ^4} (defined in (3.14)) [25]. In d spacetime dimensions, the scaling dimension of the interaction term φ^4 is

$$4 \times \frac{d-2}{2} = 2d-4$$

3.4. The Epsilon Expansion

and its upper critical dimension is 4. In other words, the methods of mean field theory are expected to break down for the physically interesting cases of $d = 1, 2, 3$. To resolve this problem, theorists promoted the parameter d to a continuous variable, and considered the model in $d = 4 - \epsilon$ dimensions for $\epsilon \ll 1$, and expanded in powers of ϵ . This was said to correspond to the theory ‘close to 4 dimensions’. Formally, this procedure of promoting d to a continuous variable is done at the level of Feynman diagrams, carrying out momentum integrals using d -dimensional spherical coordinates. The idea is that for ϵ small, the interaction is only ‘slightly’ relevant, and mean field theory might not be so bad.

In this expansion, to $\mathcal{O}(\epsilon)$, the beta function of X in (3.14) can be shown to be [26]

$$\beta_X = \epsilon X - \frac{9}{2\pi^2} X^2 \quad (3.23)$$

revealing a nontrivial fixed point $X_* = \frac{2\pi^2}{9}\epsilon$. This showcases the true power of the ϵ -expansion: the ability to search for new phase transitions that are inaccessible using mean field theory.

While we might expect the ϵ -expansion to be valid in the limit of infinitesimal ϵ , it has shown to be surprisingly predictive in the limit $\epsilon \rightarrow 1$. For example, the theory \mathcal{L}_{φ^4} , which corresponds to the classical Ising model, predicts the specific heat to scale with critical exponent $\alpha = 1/6$ at $\mathcal{O}(\epsilon)$ and $\alpha = .109$ at $\mathcal{O}(\epsilon^5)$ [26]. Even at $\mathcal{O}(\epsilon)$, the agreement with the experimental range of 0–0.14 is impressive. It is results like these that have resulted in physicists regarding the ϵ -expansion as a very important tool in the study of critical phenomena.

For the U(1) symmetric versions of (2.21) and (2.22), both the Gross-Neveu and $\mathcal{N} = 2$ SUSY critical points were identified using the ϵ -expansion (the upper critical dimension of both $\sigma\bar{\psi}\psi$ and $\phi^*\psi^T C\psi + \text{h.c.}$ is also four). These fixed points occur at the following values:[16, 27]

$$\frac{\lambda_{1,*}^2}{(4\pi)^2} = \frac{\epsilon}{12} + \mathcal{O}(\epsilon^2) \quad (3.24)$$

$$\frac{\eta_{1,*}}{(4\pi)^2} = \frac{\epsilon}{8} + \mathcal{O}(\epsilon^2) \quad (3.25)$$

To linear order in the fermion mass and the U(1) breaking couplings $\{h_i\}$, the value of these fixed points will not change, and so it makes sense to ask the following question:

What are the beta functions of M and $\{h_i\}$, evaluated at the critical points $\lambda_{1,}$ and $\eta_{1,*}$?*

We will provide an answer to this question in Chapters 4 and 5. However, in addressing this question, an issue arises involving Lorentz invariance. In the original ϵ -expansion of φ^4 theory, φ is a Lorentz scalar, transforming as a singlet under the $\text{SO}(d)$ Lorentz group in every dimension d . For a theory involving fermions, more care is needed, since not all operators invariant under $\text{SO}(3)$ are invariant under the larger $\text{SO}(4)$ Lorentz group in four dimensions. In the following section, we introduce the necessary formalism to treat these issues.

3.5 Modified Epsilon Expansion

Since the upper critical dimension of the fermion-boson interactions $\sigma\bar{\psi}\psi$ and $\phi^*\psi^T C\psi + \text{h.c.}$ is four, we will carry out an ϵ -expansion about four dimensions. In four dimensions, a two-component complex fermion is a Weyl fermion. To derive the Weyl Lagrangian, we start from the four dimensional Dirac theory in real time,

$$\mathcal{L}_D = i\bar{\Psi}\Gamma^a\partial_a\Psi. \quad (3.26)$$

The gamma matrices are in the Weyl basis, and can be written in terms of two sets of Pauli matrices $\{\sigma_i\}$ and $\{\tau_i\}$:

$$\Gamma^0 = \tau_x \otimes \sigma_0 \quad \Gamma^k = i\tau_y \otimes \sigma_k \quad (3.27)$$

where $\sigma_0 := 1$. These matrices satisfy

$$\{\Gamma^a, \Gamma^b\} = 2\text{diag}(1, -1, -1, -1). \quad (3.28)$$

Writing Ψ as

$$\Psi = (\psi_R \ \psi_L)^T \quad (3.29)$$

and expanding (3.26), the fields ψ_L and ψ_R decouple. Defining $\bar{\psi} = \psi^\dagger\sigma_y$, the ψ_L sector can be written as

$$\mathcal{L}_W = i\bar{\psi}\sigma_y\partial_0\psi + i\bar{\psi}[\sigma_y\sigma_x\partial_1 + \partial_2 + \sigma_y\sigma_z\partial_3]\psi \quad \bar{\psi} := \psi^\dagger\gamma^0 = \psi^\dagger\sigma_y \quad (3.30)$$

where we've suppressed the 'L' subscript, and inserted $\sigma_y^2 = 1$ in each term. By relabelling coordinates $\partial_2 \leftrightarrow \partial_3$, and performing a Wick rotation, we find that the imaginary time Lagrangian density for the Weyl fermion is

$$\mathcal{L}_W = \bar{\psi}[\partial_\mu\gamma^\mu + i\partial_3]\psi \quad \mu = 0, 1, 2 \quad (3.31)$$

3.5. Modified Epsilon Expansion

Since (3.31) is a Lorentz scalar, and $(\partial_\mu, \partial_3)$ is a 4-vector, we see that the object $\bar{\psi}\psi$ is no longer invariant under the Lorentz group. Instead, it is a component of the 4-vector,

$$A = \begin{pmatrix} \bar{\psi}\gamma^\mu\psi \\ \bar{\psi}\psi \end{pmatrix}, \quad (3.32)$$

that is contracted with $(\partial_\mu, \partial_3)$ in (3.31). This can also be seen explicitly, using the general form of a Lorentz transformation in the Weyl basis:[25]

$$\Lambda(\alpha) = e^{\vec{\alpha} \cdot \vec{\sigma}} \quad \vec{\alpha} \in \mathbb{C} \quad (3.33)$$

Under this transformation,

$$\bar{\psi}\psi \mapsto \psi^\dagger e^{\vec{\alpha}^* \cdot \vec{\sigma}} \gamma^0 e^{\vec{\alpha} \cdot \vec{\sigma}} \psi = \bar{\psi} e^{-\vec{\alpha}^* \cdot \vec{\sigma}^T} e^{\vec{\alpha} \cdot \vec{\sigma}} \psi \quad (3.34)$$

which does not equal $\bar{\psi}\psi$ for general $\vec{\alpha}$. It is only invariant under a subset of operators,

$$\{e^{\lambda\sigma_x}, e^{\lambda\sigma_z}, e^{i\lambda\sigma_y}\}, \quad \lambda \in \mathbb{R}$$

which generate the three dimensional Lorentz group.

The breaking of Lorentz invariance creates difficulties when studying the fermion mass operator $M\bar{\psi}\psi$, as well as the Gross-Neveu interaction $\bar{\psi}\psi\sigma$ in (2.21). While these operators are invariant under the three dimensional Euclidean Lorentz group $SO(3)$, they transform nontrivially under the full $SO(4)$ Euclidean Lorentz group. As a consequence, additional operators that are invariant only under the $SO(3) \subset SO(4)$ subgroup can be generated, including (for $k \in \mathbb{Z}_+$)

$$\bar{\psi}(i\partial_3)^k\psi \quad |\partial_3^k\phi|^2 \quad (\partial_3^k\sigma)^2 \quad (\phi\partial_3^k\phi^* + \text{h.c.}) \quad \sigma\partial_3^k\sigma \quad (3.35)$$

We will only discuss the role of the most relevant operators, with $k = 1$. Then in four dimensions, we should replace the Lagrangian densities (2.21) and (2.22) with the following:

$$\mathcal{L}'_1 = \bar{\psi}[\not{\partial} + i\partial_3 + if_1\partial_3]\psi + M\bar{\psi}\psi + (\partial_a\sigma)^2 + f_2(\partial_3\sigma)^2 + \eta_1\sigma\bar{\psi}\psi + \eta_2\sigma^4 \quad (3.36)$$

$$+ f_3\sigma\partial_3\sigma + \dots$$

$$\begin{aligned} \mathcal{L}'_2 = & \bar{\psi}[\not{\partial} + i\partial_3 + if_1\partial_3]\psi + M\bar{\psi}\psi + |\partial_a\phi|^2 + f_2|\partial_3\phi|^2 + \lambda_1[\phi\psi^T C\psi + \text{h.c.}] \\ & + \lambda_2^2|\phi|^2 + f_3(\phi\partial_3\phi^* + \text{h.c.}) + \dots \end{aligned} \quad (3.37)$$

The ‘...’ represent the U(1) breaking operators present in (2.21) and (2.22), which are unchanged. Since the parameters $\{f_i\}$ are not present in the three dimensional model, they only appear in the four dimensional model after at least one renormalization step, and are suppressed by at least one factor of M or η_1 (the Lorentz breaking operators in (3.36) and (3.37)). In either case, terms $\mathcal{O}(f_i^2)$ and $\mathcal{O}(f_i M)$ are beyond our order of approximation, and should be dropped from the calculations that follow.

3.5.1 Propagators

Inverting the quadratic forms in (3.36–3.37), we find the following propagators, to linear order in M and f_i :

$$G(p) = \langle \psi(p) \bar{\psi}(p) \rangle = \frac{i\mathbb{P} + f_1 p_3 + M}{p^2} - 2p_3(M + f_1 p_3) \frac{i\mathbb{P} + p_3}{p^4} \quad (3.38)$$

where we’ve introduced a four dimensional ‘slash notation’

$$\mathbb{A} := A_\mu \gamma^\mu - iA_3 \quad (3.39)$$

We write this propagator as a sum of a Lorentz invariant (G_1) and a non-Lorentz invariant (G_2) part:

$$G(p) = G_1(p) + G_2(p) \quad (3.40)$$

$$G_1(p) = \frac{i\mathbb{P} + M}{p^2} \quad G_2(p) = \frac{p_3}{p^2} \left[f_1 - 2(M + f_1 p_3) \frac{i\mathbb{P} + p_3}{p^2} \right] \quad (3.41)$$

Only the first term is a Lorentz invariant. Likewise, the boson propagators are

$$D(p) = \langle \sigma(p) \sigma(-p) \rangle = \langle \phi(p) \phi^*(p) \rangle = D_1 + D_2 \quad (3.42)$$

where

$$D_1(p) = \frac{1}{p^2} \quad D_2(p) = -\frac{f_2 p_3^2}{p^4} - \frac{f_3 i p_3}{p^4} \quad (3.43)$$

The presence of these non-Lorentz invariant terms in the fermion and boson propagators may seem problematic. This is because when we think of an ϵ -expansion, we usually continuously change the dimension without altering the underlying symmetries of the theory. However, this is not feasible when working with fields that transform nontrivially under the Lorentz group, such as spinors: the terms are still invariant under SO(3), but this is no longer the Lorentz group in four dimensions.

3.5. Modified Epsilon Expansion

Of course, this is not the first time an ϵ -expansion has been attempted on these models. In the case of attractive interactions, the conventional approach is to relate (2.22) to the Nambu-Jona-Lasinio model in four dimensions, involving a 4-component Majorana fermion χ , and two real bosons ϕ_1 and ϕ_2 [15, 16, 29]. The interaction term in this model is

$$\bar{\chi}(\phi_1 + i\gamma_5\phi_2)\chi \quad (3.44)$$

where γ_5 is the fifth gamma matrix in four dimensions. In the massless case, this theory possesses a continuous $U(1)$ chiral symmetry:

$$\chi \rightarrow e^{i\alpha\gamma_5}\chi \quad \phi \rightarrow e^{-2i\alpha}\phi \quad (3.45)$$

In the Majorana representation, γ_5 is pure imaginary, so that this transformation leaves the Majorana real. In three dimensions, this model corresponds to the $U(1)$ version of (2.22), with the chiral $U(1)$ mapping to the charge $U(1)$ symmetry in the three dimensional theory. However, since a Majorana mass breaks the chiral $U(1)$, we are unable to adopt this approach to our model when a fermion mass term is present.

Another popular approach in the literature, for the $U(1)$ versions of both (2.21) and (2.22), is to extend the theory to one of N Dirac fermions in four dimensions, and then continue $N \rightarrow \frac{1}{2}$ in the ϵ -expansion [16]. This approach is difficult to justify, since a four dimensional Dirac mass does not correspond to a three dimensional Dirac mass in this limit. See for instance, [30]. Instead, the four dimensional mass couples different chiral sectors together. Using a change of basis, we can decouple the sectors, but in this case the three dimensional masses occur with opposite signs, and the limit $N \rightarrow \frac{1}{2}$ is ill-defined. This is explained in more detail in Appendix B.

Therefore, we are forced to develop a new approach in order to calculate renormalization group functions in these theories. In the end, this approach will agree with the naive $N \rightarrow \frac{1}{2}$ limit in a conventional ϵ -expansion, but is arguably more reliable, since it keeps the form of all operators fixed as d is continued back to three dimensions. Perhaps there is a simple argument justifying the $N \rightarrow \frac{1}{2}$ limit, but we haven't been able to produce one.

3.5.2 An Expansion in $d = 3 + (1 - \epsilon)$ Dimensions

In this thesis, we use a different approach to extract only the Lorentz invariant contributions to our Feynman diagram calculations. It is a modified ϵ -expansion that isolates the Lorentz breaking direction (' p_3 ' in momentum space), and shrinks it to zero extent in the $\epsilon \rightarrow 1$ limit. To understand this,

3.5. Modified Epsilon Expansion

recall that the conventional ϵ -expansion is carried out at the level of internal momentum integrals. In a Lorentz invariant theory, all momentum integrals will have the structure

$$\int \frac{d^4 p}{(2\pi)^4} F(p) \quad (3.46)$$

for some function F depending only on the magnitude of momentum. Now, we continue from four to d dimensions, by writing

$$\int \frac{d^4 p}{(2\pi)^4} F(p) \rightarrow \int \frac{d^d p}{(2\pi)^d} F(p) = \Omega_d \int dp p^{d-1} F(p) \quad (3.47)$$

where Ω_d is the surface area of the sphere S_{d-1} . Both Ω_d and the radial integral are well-defined as functions of a continuous parameter d .

Now, let us turn to our non-Lorentz invariant theory, which has propagators modified by terms proportional to $\frac{p_3}{p^2}$. To lowest order in p_3^2 , any Lorentz breaking contribution to a momentum integral will have the structure

$$\int \frac{d^4 p}{(2\pi)^4} F(p) p_3^2 \quad (3.48)$$

since odd powers of p_3 vanish by the symmetric integration. Higher powers of p_3^2 will be at least quadratic in the small parameters M and f_i . In the conventional ϵ -expansion, we would now promote p to a d -dimensional vector, write $p_3^2 = p^2 F'(\theta_i)$ in terms of spherical coordinates, and find some nonzero contribution. But this is unphysical, since all Lorentz breaking contributions should vanish when we return to the three dimensional theory. Instead, we promote p to a $3 + d'$ dimensional vector, and p_3 to a d' dimensional vector, with $d' = 1 - \epsilon$:

$$\int \frac{d^4 p}{(2\pi)^4} f(p) p_3^2 \rightarrow \int \frac{d^{3+d'} p}{(2\pi)^{3+d'}} F(p) |p_3|^2 = \int \frac{d^{3+d'} p}{(2\pi)^{3+d'}} F(p) \sum_{i=3}^{2+d'} p_i^2 \quad (3.49)$$

$$= d' \int \frac{d^{3+d'} p}{(2\pi)^{3+d'}} F(p) p_1^2 = \frac{d'}{3+d'} \Omega_{3+d'} \int dp p^{3+d'+1} F(p) \quad (3.50)$$

In the limit $\epsilon \rightarrow 1$, $d' \rightarrow 0$, this integral vanishes. Since this applies to *all* Lorentz breaking contributions to the Feynman diagrams, the modified ϵ -expansion amounts to replacing the propagators in (3.40, 3.42) with their Lorentz invariant pieces, and carrying out the conventional ϵ -expansion:

$$G(p) \rightarrow G_1(p) \quad D(p) \rightarrow D_1(p) \quad (3.51)$$

Throughout the following chapters, we implement this modified scheme, and drop the subscript ‘1’ in the fermion and boson propagators.

Chapter 4

Renormalization of U(1) Breaking Operators

In this chapter, we determine the relevance of the U(1) breaking operators present in (2.21) and (2.22) to one loop order in the modified ϵ -expansion. This is done by calculating the beta functions of these operators in the Wilsonian renormalization scheme. To begin, we decompose fields into slow and fast components, following the conventions of Chapter 3. We separate the Lagrangian density into a slow, fast, and ‘mixed’ piece, according to (3.5), and keep mixed terms that have exactly two fast fields; operators with more or less fast fields do not contribute at one loop order. For the case of repulsive interactions in the Majorana model (2.21),

$$\begin{aligned} \mathcal{L}_{sf,1} = & \eta_1 \sigma_s \bar{\psi}_f \psi_f + \eta_1 \sigma_f (\bar{\psi}_s \psi_f + \bar{\psi}_f \psi_s) + 6\eta_2^2 \sigma_s^2 \sigma_f^2 + 2\sigma_s^2 \sigma_f^2 \quad (4.1) \\ & + \frac{h_1}{4} [C_{ab} C_{cd} \psi_{a,s} \psi_{b,s} \partial_r \psi_{c,f} \partial_r \psi_{d,f} + \psi_{a,f} \psi_{b,f} \partial_r \psi_{c,s} \partial_r \psi_{d,s} + \text{h.c.}] \\ & + h_1 [C_{ab} C_{cd} \psi_{a,f} \psi_{b,s} \partial_r \psi_{c,f} \partial_r \psi_{d,s} + \text{h.c.}] \end{aligned}$$

For the case of attractive interactions in the Majorana model (2.22),

$$\begin{aligned} \mathcal{L}_{sf,2} = & \lambda_2 [\phi_s^2 \phi_f^{*2} + 2|\phi_s|^2 |\phi_f|^2] + \lambda_1 C_{ab} [2\phi_f^* \psi_{a,f} \psi_{b,s} + \phi_s^* \psi_{a,f} \psi_{b,f}] \quad (4.2) \\ & + \frac{h_2}{4} C_{ab} C_{cd} [\psi_{a,s} \psi_{b,s} \partial_r \psi_{c,f} \partial_r \psi_{d,f} + \psi_{a,f} \psi_{b,f} \partial_r \psi_{c,s} \partial_r \psi_{d,s} + 4\psi_{a,f} \psi_{b,s} \partial_r \psi_{c,f} \partial_r \psi_{d,s}] \\ & + \frac{h_3}{2} C_{ab} [\phi_s \partial_r \psi_{a,f} \partial_r \psi_{b,f} + 2\phi_f \partial_r \psi_{a,f} \partial_r \psi_{b,s}] + h_4 C_{ab} [\phi_s \partial_r^2 \psi_{a,f} \psi_{b,f} + 2\phi_f \partial_r^2 \psi_{a,f} \psi_{b,s}] \end{aligned}$$

plus Hermitian conjugate terms. Integrating out the fast fields in the above theories will generate a series of Feynman diagrams, which we calculate below. These diagrams will contribute to renormalization constants Z_i , in terms of which the coupling constants are:

$$h_1 = h_{1,0} Z_{h_1} Z_\psi^{-2} b^{-d} \quad h_2 = h_{2,0} Z_{h_2} Z_\psi^{-2} b^{-d} \quad (4.3)$$

4.1. $U(1)$ Breaking Operators with Attractive Interactions

$$h_3 = h_{3,0} Z_{h_3} Z_\phi^{-1/2} b^{-d/2} \quad h_4 = h_{4,0} Z_{h_4} Z_\phi^{-1/2} b^{-d/2} \quad (4.4)$$

Above, the $\{h_{i,0}\}$ are the ‘bare’ couplings defined at scale Λ , while the $\{h_i\}$ are the couplings defined at the scale $b^{-1}\Lambda$. The explicit factors of b are generated from the rescaling (3.11). Differentiating these expressions with respect to $\log b$, we obtain the desired beta functions.

Throughout our calculations, we consider all one loop diagrams that are $\mathcal{O}(h_i)$, $\mathcal{O}(\lambda_i^2)$, $\mathcal{O}(\eta_i^2)$ and $\mathcal{O}(M)$. We define the operator $*$ on momenta vectors a, b as

$$a * b := a_x b_x - a_y b_y \quad (4.5)$$

and we use faint/bold propagator lines to denote slow/fast fields in our Feynman diagrams. We also use the notation $\mathfrak{p} := \not{p} - ip_3$, introduced in Chapter 3. From the outset, we set the boson masses to zero, since this marks the phase transitions of interest. All Feynman diagrams have been drawn using the package [31].

4.1 $U(1)$ Breaking Operators with Attractive Interactions

In this section, we evaluate the one loop diagrams corresponding to (2.22). Using the modified ϵ -expansion, the fermion and boson propagators are

$$G(p) = \frac{i\mathfrak{p} + M}{p^2} \quad D(p) = \frac{1}{p^2} \quad (4.6)$$

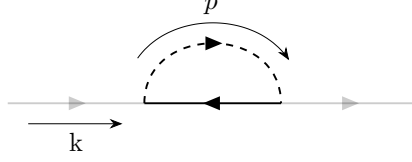
We use solid lines to represent the fermion propagators, and dashed lines to represent the boson propagators. An arrow is used to indicate the direction of charge; this charge is $+1$ for the fermion, and $+2$ for the boson. Finally, we include the operators of the external legs in the definitions of our Feynman diagrams.

4.1.1 Feynman Diagrams

Fermion Propagator

The single one loop diagram that renormalizes the fermion propagator to $\mathcal{O}(h_i)$ is shown in Figure 4.1. Including the external legs, it equals

$$= \int \frac{d^d k}{(2\pi)^d} \bar{\psi}_s(k) \Sigma_\psi(k) \psi_s(k) \quad (4.7)$$


 Figure 4.1: Fermion self energy diagram in Wilson RG for $g > 0$

where

$$\Sigma_\psi(k) = -4\lambda_1^2 \int_f \frac{d^d p}{(2\pi)^d} D(p) C^T G^T(p-k) C \quad (4.8)$$

and the p integration is over the Wilson shell. Using the modified ϵ -expansion propagators, and expanding to linear order in the slow momentum k , this is

$$\Sigma_\psi(k) = -4\lambda_1^2 \int_f \frac{d^d p}{(2\pi)^d} \frac{1}{p^2} \left[\frac{-i\mathbf{k}^\dagger - M}{p^2} + 2p \cdot k \frac{i\mathbf{p}}{p^4} \right] \quad (4.9)$$

Since the region of integration is symmetric, we can replace

$$p \cdot k i\mathbf{p}^\dagger \rightarrow \frac{p^2}{d} i\mathbf{k}^\dagger \quad (4.10)$$

to find

$$\Sigma_\psi(k) = -i\mathbf{k}^\dagger 4\lambda_1^2 \left[1 - \frac{2}{d} \right] \int_f \frac{d^d p}{(2\pi)^d} \frac{1}{p^4} - 4\lambda_1^2 M \int_f \frac{d^d p}{(2\pi)^d} \frac{1}{p^4} \quad (4.11)$$

Using

$$\int_f \frac{d^d p}{(2\pi)^d} \frac{1}{p^4} = \Omega_d \int_{b^{-1}\Lambda}^\Lambda dp p^{d-5} = \frac{2}{(4\pi)^{d/2} \Gamma(d/2)} \Lambda^{d-4} \delta l + \mathcal{O}(\delta l^2) \quad (4.12)$$

for $b = e^{\delta l}$, we find the following renormalization constants for the fermion kinetic term and fermion mass term:

$$Z_\psi = 1 + \frac{8\lambda_1^2}{(4\pi)^{d/2} \Gamma(d/2)} \left[1 - \frac{2}{d} \right] \Lambda^{-\epsilon} \delta l \quad Z_M = 1 - \frac{8\lambda_1^2}{(4\pi)^{d/2} \Gamma(d/2)} \Lambda^{-\epsilon} \delta l \quad (4.13)$$

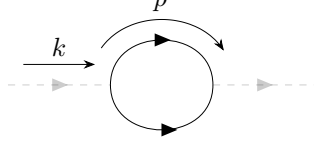


Figure 4.2: Boson self energy diagram in Wilson RG

Boson Propagator

The unique one loop diagram that renormalizes the boson propagator to linear order in $\mathcal{O}(h_i)$ is shown in Figure 4.2. It equals

$$= \int \frac{d^d k}{(2\pi)^d} \phi_s^*(k) \Sigma_\phi(k) \phi_s(k) \quad (4.14)$$

where

$$\Sigma_\phi(k) = 2\lambda_1^2 \int_f \frac{d^d p}{(2\pi)^d} \text{tr}[CG(p)CG^T(k-p)] \quad (4.15)$$

Using

$$= CG^T(p)C = \frac{i\mathfrak{P} - M}{p^2} \quad (4.16)$$

we have

$$\Sigma_\phi(k) = 2\lambda_1^2 \int_f \frac{d^d p}{(2\pi)^d} \frac{1}{p^2(k-p)^2} \text{tr}[(i\mathfrak{P} + M)(i\mathfrak{k}^\dagger - \mathfrak{P}^\dagger - M)] \quad (4.17)$$

Since the phase transition occurs when the boson mass is tuned to zero, we isolate the terms proportional to k^2 , to extract Z_ϕ . We need not be concerned with the generation of terms proportional to k_4 only, since these drop out of the modified ϵ -expansion. We find

$$Z_\phi = 1 + \frac{8}{(4\pi)^{d/2}\Gamma(d/2)} \left[1 - \frac{2}{d}\right] \lambda_1^2 \Lambda^{-\epsilon} \delta l. \quad (4.18)$$

Renormalization of h_2

At one loop, there is no diagram renormalizing h_2 . Therefore,

$$Z_{h_2} = 1 \quad (4.19)$$

Renormalization of h_3 and h_4 :

There are two diagrams that contribution to the renormalization of h_3 and h_4 at one loop. The first is shown in Figure 4.3, and equals

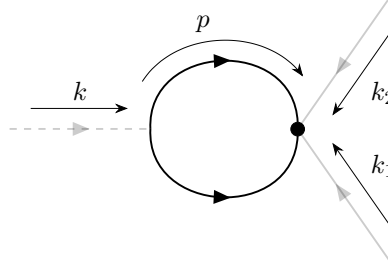


Figure 4.3: First diagram renormalizing h_3 and h_4 in Wilson RG.

$$= \int \frac{d^d k_1}{(2\pi)^d} \frac{d^d k_2}{(2\pi)^d} \phi_s(-k_1 - k_2) \psi_{a,s}(k_1) F_{ab}(k_1, k_2) \psi_{b,s}(k_2) \quad (4.20)$$

where $k := -k_1 - k_2$, the solid vertex denotes an insertion of the $U(1)$ breaking operator h_2 , and

$$F(k_1, k_2) = -\frac{\lambda_1 h_2}{2} \int_f d^d p \left[C[p * (k-p) + k_1 * k_2] \text{tr}[CG(p)CG^T(k-p)] \right. \\ \left. - 4k_2 * (k-p)CG(p)CG^T(k-p)C \right] \quad (4.21)$$

The integrand of this expression is, to $\mathcal{O}(M)$,

$$-2C \frac{[p * (k-p) + k_1 * k_2]}{p^2(k-p)^2} p \cdot (k-p) + \frac{4k_2 * (k-p)C}{p^2(k-p)^2} [p \cdot (k-p) + iM(\mathbf{p} - \mathbf{k}^\dagger + \mathbf{p}^\dagger)] \quad (4.22)$$

where we've dropped terms according to the modified ϵ -expansion procedure. In spherical coordinates,

$$p * p = p_x^2 - p_y^2 = p^2 \sin \theta \cos(2\phi) \quad (4.23)$$

integrates to zero over angular coordinates when multiplied by any power of $|p|$, so we can drop such terms. Likewise, $(p * k)p$ integrates to zero since it

4.1. $U(1)$ Breaking Operators with Attractive Interactions

is odd in p_z . Keeping at most two powers of slow momenta k , and dropping terms that vanish upon integration, we can replace the previous expression with

$$2C \frac{3k_1 * k_2 + 2k_2 * k_2}{p^2} \quad (4.24)$$

so that

$$F(k_1, k_2) = -\lambda_1 h_2 C [3k_1 * k_2 + 2k_2 * k_2] \int_f d^d p \frac{1}{p^2} \quad (4.25)$$

$$= -\lambda_1 h_2 C [3k_1 * k_2 + 2k_2 * k_2] \frac{2}{(4\pi)^{d/2} \Gamma(d/2)} \Lambda^{d-2} \delta l \quad (4.26)$$

The second diagram renormalizing h_3 and h_4 is shown in Figure 4.4, and equals

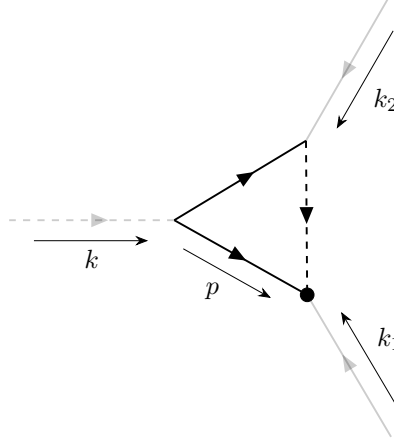


Figure 4.4: Second diagram renormalizing h_3 and h_4 in Wilson RG

$$\int \frac{d^d k_1}{(2\pi)^d} \frac{d^d k_2}{(2\pi)^d} \phi_s(-k_1 - k_2) \psi_{a,s}(k_1) G_{ab}(k_1, k_2) \psi_{b,s}(k_2) \quad (4.27)$$

where $k := -k_1 - k_2$, and the solid vertex denotes the insertion of the $U(1)$ breaking operators proportional to h_3 and h_4 , and

$$G(k_1, k_2) = -4\lambda_1^2 \int_f \frac{d^d p}{(2\pi)^d} D(p) C G(p - k_1) C G^T(-p - k_2) \quad (4.28)$$

4.1. $U(1)$ Breaking Operators with Attractive Interactions

$$\times [h_3 k_2 * (-p - k_2) + 2h_4(p + k_2) * (p + k_2)]$$

Again, we drop terms proportional to $p * p$ and $k * p$, since they will integrate to zero. The result is, to quadratic order in the slow momenta k ,

$$G(k_1, k_2) \rightarrow -4(2h_4 - h_3)k_2 * k_2 \lambda_1^2 \int_f \frac{d^d p}{(2\pi)^d} D(p) C G(p - k_1) C G^T(-p - k_2) \quad (4.29)$$

$$= -4(2h_4 - h_3)k_2 * k_2 \lambda_1^2 C \int_f \frac{d^d p}{(2\pi)^d} \frac{1}{p^4} \quad (4.30)$$

$$= -4(2h_4 - h_3)k_2 * k_2 \lambda_1^2 C \frac{2}{(4\pi)^{d/2} \Gamma(d/2)} \Lambda^{-\epsilon} \delta l \quad (4.31)$$

Adding this result to (4.25), we find the following renormalization constants:

$$Z_{h_3} = 1 - \frac{6\lambda_1 h_2}{h_3} \frac{2\Lambda^{-\epsilon} \delta l}{(4\pi)^{d/2} \Gamma(d/2)} \quad (4.32)$$

and

$$Z_{h_4} = 1 + [2\lambda_1 h_2 + 4(2h_4 - h_3)\lambda_1^2] \frac{2\Lambda^{-\epsilon} \delta l}{(4\pi)^{d/2} \Gamma(d/2) h_4} \quad (4.33)$$

The factors of Λ^2 were removed by redefining the couplings constants to be dimensionless from the start of the calculation.

Remaining Diagrams

For all remaining diagrams, we cite the calculations of [27], since these do not receive corrections from the $U(1)$ breaking terms or the fermion mass to this order. As a result, the beta functions for λ_1 and λ_2 are unchanged, and we can use the critical value $\lambda_{1,*}^2$ from [27]:

$$\frac{\lambda_{1,*}^2}{(4\pi)^2} = \frac{\epsilon}{12} + \mathcal{O}(\epsilon^2) \quad (4.34)$$

Renormalization Constants at $\mathcal{O}(\epsilon)$

To determine the value of these renormalization constants to $\mathcal{O}(\epsilon)$, we replace λ_1^2 in these expressions with $\lambda_{1,*}$ in (4.34). Any corrections from $U(1)$

4.1. $U(1)$ Breaking Operators with Attractive Interactions

breaking operators or the fermion mass will be higher order in the parameters $\{h_i, M\}$. We find, to $\mathcal{O}(\epsilon)$, the following renormalization coefficients:

$$Z_\psi = 1 + \frac{\epsilon}{3}\delta l \quad (4.35)$$

$$Z_M = 1 - \frac{2\epsilon}{3}\delta l \quad (4.36)$$

$$Z_{h_2} = 1 \quad (4.37)$$

$$Z_{h_3} = 1 - \frac{6h_2\delta l}{h_3\sqrt{3}(4\pi)}\sqrt{\epsilon} \quad (4.38)$$

$$Z_{h_4} = 1 + 2\delta l \left[\frac{h_2\sqrt{\epsilon}}{h_4 4\pi\sqrt{3}} + \frac{\epsilon(2h_4 - h_3)}{3h_4} \right] \quad (4.39)$$

$$(4.40)$$

4.1.2 Beta Functions of $U(1)$ Breaking Operators

Using (4.3 - 4.4), we find

$$\beta_M = M \left[1 + \frac{dZ_M}{d\delta l} - \frac{dZ_\psi}{d\delta l} \right] = M [1 - \epsilon] \quad (4.41)$$

$$\beta_{h_2} = -h_2 \left[d + 2 \frac{dZ_\psi}{d\delta l} \right] = -h_2 \left[4 - \frac{\epsilon}{3} \right] \quad (4.42)$$

$$\beta_{h_3} = -h_3 \left[\frac{d}{2} + \frac{3}{2} \frac{dZ_\psi}{d\delta l} - \frac{d\delta Z_{h_3}}{d\delta l} \right] = -h_3 \left[2 + \frac{6h_2\sqrt{\epsilon}}{\sqrt{3}(4\pi)h_3} \right] \quad (4.43)$$

$$\beta_{h_4} = -h_4 \left[\frac{d}{2} + \frac{3}{2} \frac{dZ_\psi}{d\delta l} - \frac{d\delta Z_{h_4}}{\delta l} \right] = -h_4 \left[2 - \frac{2h_2\sqrt{\epsilon}}{h_4 4\pi\sqrt{3}} - \frac{2\epsilon(2h_4 - h_3)}{3h_4} \right] \quad (4.44)$$

$$(4.45)$$

Since β_{h_2} is only a function of h_2 , and is negative for $\epsilon = 1$, we conclude that h_2 flows to zero at large length scales, independent of h_3 and h_4 . This implies that β_{h_3} is also negative at large length scales, so that $h_3 \rightarrow 0$. Finally, we are left with

$$\beta_{h_4} \rightarrow -h_4 \left[2 - \frac{4\epsilon}{3} \right] \rightarrow -\frac{2}{3}h_4 < 0 \quad (4.46)$$

so that h_4 also flows to zero. Therefore, at the critical point $g_{c,2}$, all $U(1)$ breaking operators are irrelevant. Meanwhile, the fermion mass operator is marginal at one loop, and requires a higher order calculation. In the next chapter, we set the $U(1)$ breaking operators to zero, and carry out a four loop study to address the relevance of a fermion mass.

4.2 $U(1)$ Breaking Operators with Repulsive Interactions

We now calculate the renormalization constants for the theory (2.21). In this case, the only $U(1)$ breaking operator is a four-fermi term. According (4.3), to determine the h_1 beta function, we only have to calculate Z_ψ and Z_{h_1} . Since there is no one loop diagram renormalizing h_1 , calculating the fermion propagator will be sufficient. Note that we are using the same symbol Z_ψ for the renormalization constant in both (2.21) and (2.22), even though they are different quantities.

Using the modified ϵ -expansion, the fermion and boson propagators are

$$G(p) = \frac{i\mathbb{P}}{p^2} \quad D(p) = \frac{1}{p^2} \quad (4.47)$$

The fermion mass is set to zero since time reversal symmetry is present at the transition $g_{c,1}$. We use solid lines (with an arrow indicating the direction of charge) to represent the fermion propagators, and dashed lines to represent the boson propagators. As before, we include the operators of the external legs in the definitions of our Feynman diagrams.

4.2.1 Feynman Diagrams

Fermion Propagator

The single one loop diagram that renormalizes the fermion propagator to $\mathcal{O}(h_1)$ is shown in Figure 4.5. It equals

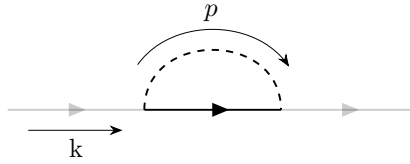


Figure 4.5: Fermion self energy in Wilson RG for $g < 0$

$$= \int \frac{d^d k}{(2\pi)^d} \bar{\psi}_s(k) \Sigma_\psi(k) \psi_s(k) \quad (4.48)$$

4.2. $U(1)$ Breaking Operators with Repulsive Interactions

where

$$\Sigma_\psi(k) = \eta_1^2 \int \frac{d^d p}{(2\pi)^d} D(p) G(k+p) \quad (4.49)$$

We expand $\Sigma_\psi(k)$ in powers of k , and extract the linear piece to determine Z_ψ :

$$\Sigma_\psi(k) = \eta_1^2 \int \frac{d^d p}{(2\pi)^d} D(p) G(k+p) \rightarrow \int \frac{d^d p}{(2\pi)^d} \frac{1}{p^2} \left[\frac{i\mathbf{k}}{p^2} - 2p \cdot k \frac{i\mathbf{p}}{p^4} \right] \quad (4.50)$$

$$= \eta_1^2 \left[1 - \frac{2}{d} \right] (i\mathbf{k}) \int \frac{d^d p}{(2\pi)^d} \frac{1}{p^4} = \eta_1^2 \left[1 - \frac{2}{d} \right] (i\mathbf{k}) \frac{2\Lambda^{-\epsilon} \delta l}{(4\pi)^{d/2} \Gamma(d/2)} \quad (4.51)$$

so that

$$Z_\psi = 1 + \left[1 - \frac{2}{d} \right] \frac{2\eta_1^2 \Lambda^{-\epsilon}}{(4\pi)^{d/2} \Gamma(d/2)} \quad (4.52)$$

where we've replaced \mathbf{k} with \mathbf{k}^\dagger , since the difference renormalizes the operator $\bar{\psi} k_3 \psi$, which doesn't enter into the modified ϵ -expansion.

Since the beta functions for η_1, η_2 receive no $\mathcal{O}(h_1)$ corrections, we can cite the results of [16] that at the critical point $g_{c,1}$, η_1 has a value of

$$\frac{\eta_{1,*}^2}{(4\pi)^2} = \frac{\epsilon}{8} + \mathcal{O}(\epsilon^2) \quad (4.53)$$

so that to $\mathcal{O}(\epsilon)$,

$$Z_\psi = 1 + \frac{\eta_1^2}{(4\pi)^2} = 1 + \frac{\epsilon}{8} \quad (4.54)$$

4.2.2 Beta Functions of $U(1)$ Breaking Operator

Using (4.3), we find

$$\beta_{h_1} = -h_1 \left[4 - \frac{3}{4}\epsilon \right] \quad (4.55)$$

at the phase transition $g_{c,1}$. Therefore, to one loop order, the $U(1)$ breaking operator is irrelevant, and the phase transition falls into the Gross-Neveu universality class, as predicted in [10].

Chapter 5

Relevance of the Fermion Mass Operator

In this chapter, we determine the relevance of the fermion mass operator in (2.22) beyond one loop order in the modified ϵ -expansion. We treat M as a small parameter, so that terms $\mathcal{O}(M^2)$ will be dropped. We also neglect all U(1) breaking operators, since these were shown to be irrelevant in the previous section.

A straightforward, but tedious approach to the problem is to calculate all two loop diagrams in the modified ϵ -expansion. This is done in Appendix C. A more efficient approach is to relate the fermion mass beta function to the *stability critical exponent* in the massless theory, which allows us to go to $\mathcal{O}(\epsilon^4)$, using the following identity:

$$\beta_M = M [1 - \omega] \quad \omega := \frac{d}{d\lambda_1^2} \frac{d\lambda_1^2}{d \log \mu} \Big|_{\lambda_1 = \lambda_1^*, (\text{massless})} \quad (5.1)$$

In words, ω is the derivative of the beta function for λ_1^2 , in the massless theory, evaluated at the critical point. To prove equation (5.1), we first develop the superspace formalism. This argument closely follows the derivation of the identity

$$\beta_{m^2} = m[2 - \omega] \quad (5.2)$$

for the boson mass operator $m^2|\phi|^2$ in [27]. The identity (5.2) was first claimed in [11]).

5.1 The Power of Supersymmetry

In this section, we derive (5.1) for the theory (2.22) at the critical point $g_{c,2}$, where the two U(1) invariant couplings λ_1 and λ_2 flow to a common value, λ_* [27]. We use the results of Chapter 4 to ignore all U(1) breaking operators, so that the theory is supersymmetric in the massless limit.

5.1.1 Superspace Formalism

Our first step will be to rewrite the massless theory (2.22) in the superspace formalism. This is most easily done in real time. We introduce a chiral superfield

$$\Phi(y) := \phi(y) + \sqrt{2}\theta\psi(y) + \theta^2 F(y) \quad (5.3)$$

where $\theta, \bar{\theta}$ are two-component Grassmann spinors, and y is the (real time) superspace coordinate

$$y^\mu := x^\mu - i\theta\gamma_R^\mu\bar{\theta} \quad (5.4)$$

By real time, we mean that x^μ is a real time coordinate, and the matrices $\gamma_R^\mu = \{-\gamma^0, i\gamma^1, i\gamma^2\}$ satisfy the 2+1 dimensional Minkowski metric:

$$\{\gamma_R^\mu, \gamma_R^\nu\} = 2\text{diag}(1, -1, -1) \quad (5.5)$$

Throughout, we use the following spinor summation convention:

$$\theta^\alpha = \epsilon^{\alpha\beta}\theta_\beta \quad \theta_\alpha = \epsilon_{\alpha\beta}\theta^\beta \quad \theta^2 = \theta^\alpha\theta_\alpha = 2\theta_2\theta_1 \quad (5.6)$$

where

$$\epsilon_{\alpha\beta} := \begin{pmatrix} 0 & -1 \\ 1 & 0 \end{pmatrix} \quad \epsilon^{\alpha\beta} := \begin{pmatrix} 0 & 1 \\ -1 & 0 \end{pmatrix} \quad (5.7)$$

Within this convention, we have the following identities

$$\theta_\alpha\theta_\beta = \theta^\alpha\theta^\beta = \frac{1}{2}\theta^2\epsilon_{\alpha\beta} \quad \theta\gamma_R^\mu\bar{\theta}\theta\gamma_R^\nu\bar{\theta} = \frac{1}{4}\theta^2\bar{\theta}^2\text{tr}[\gamma_R^\mu\gamma_R^\nu] = \frac{1}{4}\theta^2\bar{\theta}^2\eta^{\mu\nu} \quad (5.8)$$

Finally, the Grassmann integration measure is defined as follows:

$$d^2\theta = -\frac{1}{4}d\theta^\alpha d\theta^\beta \epsilon_{\alpha\beta} \quad \implies \quad \int d^2\theta\theta^2 = 1 \quad (5.9)$$

Using this formalism, the superfield can be expanded as

$$\Phi(y) = \phi(x) - i\theta\gamma_R^\mu\bar{\theta}\partial_\mu\phi(x) - \frac{1}{4}\theta^2\bar{\theta}^2\partial^\mu\partial_\mu\phi + \sqrt{2}\theta\psi(x) + \frac{i\theta^2}{\sqrt{2}}\partial_\mu\psi(x)\gamma_R^\mu\bar{\theta} + \theta^2 F(x). \quad (5.10)$$

where $\partial_R^2 := \partial_\mu\partial_\nu\eta^{\mu\nu}$.

Using this, the free SUSY Lagrangian density is

$$\begin{aligned} \mathcal{L}_{\text{SUSY}}^0 = \int d^2\theta d^2\bar{\theta} \Phi^\dagger \Phi = & -\frac{1}{4}[\partial_R^2\phi\phi^* + \phi\partial_R^2\phi^*] + |F|^2 + \frac{1}{2}\partial_\mu\phi\partial_\nu\phi^*\eta^{\mu\nu} \\ & + i \int d^2\bar{\theta}\theta\bar{\psi}\partial_\mu\psi\gamma_R^\mu\bar{\theta} - i \int d^2\theta\theta\gamma_R^\mu\partial_\mu\bar{\psi}\theta\psi \end{aligned} \quad (5.11)$$

5.1. The Power of Supersymmetry

Since

$$\bar{\theta}\partial_\mu\gamma_R^\mu\bar{\theta} = \frac{1}{2}\bar{\theta}^2\bar{\psi}\gamma_R^{\mu,T}\partial_\mu\psi \quad \theta\gamma^\mu\partial_\mu\bar{\psi}\theta\psi = -\frac{1}{2}\theta^2\bar{\psi}\gamma^{\mu,T}\partial_\mu\psi \quad (5.12)$$

up to total derivatives, equation (5.11) equals

$$|F|^2 + \partial_\mu\phi^*\partial_\nu\eta^{\mu\nu}\phi + i\bar{\psi}\gamma_R^{\mu,T}\partial_\mu\psi \quad (5.13)$$

To produce a boson-fermion interaction term, we add to (5.11) a superpotential term

$$\delta\mathcal{L}_{\text{SUSY}} = \int d^2\theta W(\Phi) + \int d^2\bar{\theta} W(\Phi^\dagger) \quad W(\Phi) := \frac{\lambda}{3}\Phi^3 \quad (5.14)$$

and apply the equations of motion for the auxiliary field F :

$$F = -\lambda\phi^{*2} \quad F^* = -\lambda\phi^2 \quad (5.15)$$

We find, using $\theta\psi\theta\psi = -\frac{1}{2}\psi^T[i\sigma_2]\psi$, that

$$\mathcal{L}_{\text{SUSY}} := \mathcal{L}_{\text{SUSY}}^0 + \delta\mathcal{L}_{\text{SUSY}} = \partial_\mu\phi^*\partial_\nu\eta^{\mu\nu}\phi + i\bar{\psi}\gamma_R^\mu\partial_\mu\psi - \lambda^2|\phi|^4 - \lambda(\phi\psi^TC\psi + \text{h.c.}) \quad (5.16)$$

which is exactly the real time version of (2.22), at the critical point $\lambda_1 = \lambda_2 = \lambda \equiv \lambda_*$. In other words:

$$\int d^2\theta d^2\bar{\theta}\Phi^\dagger\Phi + \int d^2\theta\frac{\lambda}{3}\Phi^3 + \int d^2\bar{\theta}\frac{\lambda}{3}\Phi^{\dagger 3} = \mathcal{L}_{2,\text{real}} \quad (5.17)$$

5.1.2 Relating the fermion beta function and the stability critical exponent

Now that we've rewritten (the real time version of) \mathcal{L}_2 in the superspace formalism, we would like to introduce a fermion mass operator in this language. This is achieved by adding the following expression to (5.17):

$$-\int d^2\theta d^2\bar{\theta} 2M\Phi^\dagger\theta\bar{\theta}\Phi = -4M\int d^2\theta d^2\bar{\theta}\bar{\psi}\theta\bar{\theta}\theta\psi = -M\bar{\psi}\psi \quad (5.18)$$

To linear order in M , this addition can be compensated by rescaling the superfield,

$$\Phi \rightarrow (1 + M\theta\bar{\theta})\Phi \quad (5.19)$$

which shifts the coupling λ accordingly:

$$\lambda \rightarrow \tilde{\lambda}(M) := \lambda + 3M\theta\bar{\theta} \quad (5.20)$$

5.1. The Power of Supersymmetry

In other words, the massive theory with coupling λ is equivalent to the massless theory with coupling $\tilde{\lambda}$. Now, to access the scaling dimension of $\bar{\psi}\psi$, we require the notion of bare and renormalized fields and masses. We write the bare theory in terms of bare Φ_0 and bare M_0, λ_0 :

$$\mathcal{L}_{\text{bare}} = \int d^2\theta d^2\bar{\theta} \Phi_0^\dagger (1 - 2M_0\theta\bar{\theta}) \Phi_0 + \int d^2\theta \frac{\lambda_0}{3} \Phi_0^3 + \int d^2\bar{\theta} \frac{\lambda_0}{3} [\Phi_0^\dagger]^3 \quad (5.21)$$

and the renormalized theory in terms of Φ and $M\mu, \lambda\mu^{\epsilon/2}$:

$$\mathcal{L} = \int d^2\theta d^2\bar{\theta} \tilde{Z} \Phi^\dagger (1 - 2M\mu\theta\bar{\theta}) \Phi + \int d^2\theta \frac{\lambda\mu^{\epsilon/2}}{3} \Phi^3 + \int d^2\bar{\theta} \frac{\lambda\mu^{\epsilon/2}}{3} [\Phi^\dagger]^3 \quad (5.22)$$

Here the renormalization scale μ has been introduced so that M and λ are dimensionless. Notice that there is no renormalization constant Z_λ – this follows from SUSY nonrenormalization theorems [32, 33]. In the massless theory, we can write down an equation similar to (5.22), replacing \tilde{Z} with some other renormalization constant Z . In general, these two functions will be different; however, using (5.20), we have

$$\tilde{Z}(\lambda) = Z(\tilde{\lambda}) = Z(\lambda) \left[1 + 3M\mu\theta\bar{\theta}\lambda \frac{\partial \log Z}{\partial \lambda} \right] + \mathcal{O}(M^2) \quad (5.23)$$

Using this and comparing (5.21) to (5.22), and we find the relation

$$M = M_0\mu^{-1} \left[1 - \frac{3}{2}\lambda \frac{\partial \log Z}{\partial \lambda} \right]^{-1} \quad (5.24)$$

Writing

$$\lambda \frac{\partial \log Z}{\partial \lambda} = 2\lambda^2 \frac{\partial \log Z}{\partial \lambda^2} \quad (5.25)$$

to expand

$$\left[1 - \frac{3}{2}\lambda \frac{\partial \log Z}{\partial \lambda} \right]^{-1} = 1 + 3\lambda^2 \frac{\partial^2 \log Z}{\partial \lambda^2} + \mathcal{O}(\lambda^4), \quad (5.26)$$

we can differentiate (5.24) with respect to $\log \mu$ to find

$$-\beta_M := \frac{\partial M}{\partial \log \mu} = M \left[-1 - 3\lambda^2 \frac{\partial \gamma}{\partial \lambda^2} \right] \quad (5.27)$$

where $\gamma = -\frac{\partial Z}{\partial \log \mu}$ is the anomalous dimension of the fermion in the massless theory. The unconventional negative sign is introduced so that these functions agree with their Wilson counterparts. Now, in the supersymmetric theory, γ can be rewritten in terms of the beta function of λ^2 , since

$$\lambda_0^2 = \lambda^2 \mu^{-\epsilon} Z(\lambda)^3 \quad (5.28)$$

because the superpotential is not renormalized. The beta function is

$$-\beta_{\lambda^2} = -\frac{d\lambda^2}{d\log\mu} = \lambda^2[-\epsilon - 3\gamma] \quad (5.29)$$

Differentiating with respect to λ^2 , and using the fact that to $\mathcal{O}(\epsilon^4)$, the value of γ at the SUSY point ($=: \lambda_*$) is ([29])

$$\gamma(\lambda_*) = -\frac{\epsilon}{3} \quad (5.30)$$

we have

$$-\frac{d\beta_{\lambda^2}}{d\lambda^2} = -\epsilon - 3\gamma(\lambda_*) - 3\lambda_*^2 \frac{\partial\gamma}{\partial\lambda^2} = -3\lambda_*^2 \frac{\partial\gamma}{\partial\lambda^2} \quad (5.31)$$

Comparing this to (5.27), we find

$$\beta_M = M \left[1 - \frac{d\beta_{\lambda^2}}{d\lambda^2} \right] \quad (5.32)$$

proving (5.1).

5.2 Fermion Mass Beta Function

In [29], ω has been evaluated in the massless theory to four loop order:

$$\omega = \epsilon - \frac{\epsilon^2}{3} + \left(\frac{1}{18} + \frac{2\zeta_3}{3} \right) \epsilon^3 + \frac{1}{540} (420\zeta_3 + 1200\zeta_5 - 3\pi^4 + 35) \epsilon^4 + \mathcal{O}(\epsilon^5) \quad (5.33)$$

Using Padé extrapolation (see [16]), the authors of [29] found the values $\omega = 0.872$ and $\omega = 0.870$, depending on which Padé approximant is used. In [34], the value $\omega = .910$ was obtained using the conformal bootstrap. In all three approaches,

$$\beta_M = M [1 - \omega] \quad (5.34)$$

is positive, and the fermion mass operator is relevant. Therefore, at the phase transition $g_{c,2}$, a time reversal breaking perturbation will destroy the emergent supersymmetry. The resulting universality class is determined in the following subsection. However, if time reversal is an approximate symmetry of the underlying lattice model, some signatures of supersymmetry, including equal scaling dimensions for the boson and fermion fields, may still be present. In passing, we note that our explicit two loop results, calculated using dimensional regularization, agree with (5.1) and (5.33) to $\mathcal{O}(\epsilon^2)$ (see Appendix C).

5.3 Consequence of a Relevant Fermion Mass Operator

Since the fermion mass is relevant, a large mass will be generated near the critical point. At energy scales $\ll M$, the fermion degrees of freedom can be integrated out completely. To perform this integration explicitly, we use a Hubbard-Stratonovich transformation to replace *all* of the four-Fermi interactions in (2.17) with

$$\mathcal{L}_{\text{int}} = -m^2|\phi|^2 + (\phi[\rho_1\bar{\psi}C\bar{\psi}^T + \rho_2\partial_r\psi^TC\partial_r\psi] + \text{h.c.}) \quad (5.35)$$

where

$$\rho_1 = 4m\sqrt{g}\Lambda_0^{-1} \quad \rho_2 = \frac{m}{2} \frac{\sqrt{g}}{\Lambda_0^3} \quad (5.36)$$

This expression (5.35) reproduces (2.17) to $\mathcal{O}(g)$ when ϕ is integrated out. The boson ϕ no longer corresponds to the Cooper pair $\phi \sim \psi_1\psi_2$ of (2.22); instead, it corresponds to

$$\phi \sim \psi_1\psi_2 + \frac{1}{2}\partial_r\psi_1^*\partial_r\psi_2^*. \quad (5.37)$$

We can use (5.37) to determine how ϕ transforms under the exact lattice symmetries (2.25 - 2.27). Explicitly, these transformations are

$$C : \quad \phi(x, y) \mapsto \phi^*(x, y) \quad (5.38)$$

$$T : \quad \phi(x, y) \mapsto -\phi^*(x, y), \quad i \mapsto -i \quad (5.39)$$

$$P : \quad \phi(x, y) \mapsto \phi^*(-x, y) \quad (5.40)$$

$$R : \quad \phi(x, y) \mapsto i\phi(-y, x) \quad (5.41)$$

The most noteworthy equation is (5.41), since it implies that the most relevant U(1) breaking operator allowed by symmetry is $\phi^4 + \phi^{*4}$. To determine the coefficient of this operator, we integrate out the fermions explicitly, using the notation introduced in Chapter 4. The unique one loop diagram generating a ϕ^4 interaction is shown in Figure 5.1. We are not interested in derivative operators, so we can set all external momenta to zero. The contribution to the operator ϕ^4 is then equal to

$$= -8\rho_1^2\rho_2^2 \int \frac{d^3p}{(2\pi)^3} (p * p)^2 \text{tr}[G(p)CG^T(-p)CG(p)CG^T(-p)C] \quad (5.42)$$

where the integral is over all momentum modes up to a cutoff $\Lambda \sim M$. Using $C(\not{p}^T + M)C = \not{p} - M$, the trace equals

$$\text{tr}[G(p)CG^T(-p)CG(p)CG^T(-p)C] = \frac{2}{(p^2 + M^2)^2} \quad (5.43)$$

5.3. Consequence of a Relevant Fermion Mass Operator

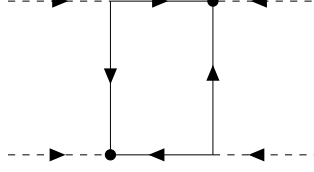


Figure 5.1: Diagram generating $\phi^4 + \text{h.c.}$ when the fermion mass is relevant

Writing $p * p = p^2 \sin^2 \theta \cos(2\phi)$ in spherical coordinates, the expression (5.42) equals

$$-16\rho_1^2\rho_2^2 \int \frac{d^3p}{(2\pi)^3} \frac{p^4 \sin^4 \theta \cos^2(2\phi)}{(p^2 + M^2)^2} \propto \rho_1^2\rho_2^2 M^3 \quad (5.44)$$

Therefore, a $\phi^4 + \text{h.c.}$ operator is generated, with coupling constant proportional to

$$\rho_1^2\rho_2^2 M^3 \propto \Lambda_0^{-1} \left(\frac{m}{\Lambda_0}\right)^4 g^2 \left(\frac{M}{\Lambda_0}\right)^3 \quad (5.45)$$

Since our original assumption was that the fermion mass is small compared to the bare cutoff, we see that the coefficient of ϕ^4 is highly suppressed. Therefore, the low energy theory near the critical point $g_{c,2}$ has the following structure

$$\mathcal{L} = |\partial_\mu \phi|^2 + m^2 |\phi|^2 + \rho |\phi|^4 + \tilde{\rho}(\phi_4 + \phi_4^*) \quad \tilde{\rho} \ll \rho \quad (5.46)$$

This model was studied in [35, 36] using ϵ -expansion techniques and in [37] using Monte Carlo, where it was shown that $\tilde{\rho}$, which lowers the symmetry from $U(1)$ to Z_4 , is irrelevant in 3 spacetime dimensions and the critical point is the XY one. Therefore, once the fermion mass becomes relevant, the universality class of $g_{c,2}$ will change from $\mathcal{N} = 2$ SUSY to the conventional XY transition.

Chapter 6

Conclusion

In this work, we have shown that the emergent $U(1)$ symmetry present at the critical points of the Majorana-Hubbard model is preserved when $U(1)$ breaking corrections are taken into account. Moreover, we have shown that a fermion mass term, generated by a time reversal breaking perturbation, is a relevant operator at four loops in the ϵ -expansion. These results suggest that in the case of repulsive interactions, the Majorana-Hubbard model has a critical point in the Gross-Neveu universality class, and in the case of attractive interactions, the model has a critical point in the $\mathcal{N} = 2$ supersymmetric universality class when time reversal symmetry is unbroken, and in the XY universality class otherwise. These results agree with the classification of Affleck et. al.[10]. Numerical confirmation of these predictions remains a major open challenge.

Bibliography

- [1] P. A. M. Dirac. The Quantum Theory of the Electron. *Proceedings of the Royal Society of London Series A*, 117:610–624, February 1928.
- [2] Steven R. Elliott and Marcel Franz. Colloquium: Majorana fermions in nuclear, particle, and solid-state physics. *Rev. Mod. Phys.*, 87:137–163, Feb 2015.
- [3] C. D. Anderson. The Positive Electron. *Physical Review*, 43:491–494, March 1933.
- [4] Jason Alicea. New directions in the pursuit of majorana fermions in solid state systems. *Reports on Progress in Physics*, 75(7):076501, 2012.
- [5] CWJ Beenakker. Search for majorana fermions in superconductors. *Annu. Rev. Condens. Matter Phys.*, 4(1):113–136, 2013.
- [6] A. Rahmani, X. Zhu, M. Franz, and I. Affleck. Emergent Supersymmetry from Strongly Interacting Majorana Zero Modes. *Physical Review Letters*, 115(16):166401, October 2015.
- [7] A. Rahmani, X. Zhu, M. Franz, and I. Affleck. Phase diagram of the interacting Majorana chain model. *Phys. Rev. B*, 92(23):235123, December 2015.
- [8] A Milsted, L Seabra, IC Fulga, CWJ Beenakker, and E Cobanera. Statistical translation invariance protects a topological insulator from interactions. *Physical Review B*, 92(8):085139, 2015.
- [9] Ching-Kai Chiu, DI Pikulin, and M Franz. Strongly interacting majorana fermions. *Physical Review B*, 91(16):165402, 2015.
- [10] Ian Affleck, Armin Rahmani, and Dmitry Pikulin. Majorana-hubbard model on the square lattice. *Phys. Rev. B*, 96:125121, Sep 2017.
- [11] S. Thomas. Emergent supersymmetry. *seminar at KITP*, 2005.

- [12] S.-S. Lee. Emergence of supersymmetry at a critical point of a lattice model. *Phys. Rev. B*, 76:075103, 2007.
- [13] Pedro Ponte and Sung-Sik Lee. Emergence of supersymmetry on the surface of three-dimensional topological insulators. *New Journal of Physics*, 16(1):013044, 2014.
- [14] Shao-Kai Jian, Yi-Fan Jiang, and Hong Yao. Emergent spacetime supersymmetry in 3d weyl semimetals and 2d dirac semimetals. *Phys. Rev. Lett.*, 114:237001, Jun 2015.
- [15] N. Zerf, C.-H. Lin, and J. Maciejko. Superconducting quantum criticality of topological surface states at three loops. *Phys. Rev. B*, 94:205106, 2016.
- [16] Lin Fei, Simone Giombi, Igor R. Klebanov, and Grigory Tarnopolsky. Yukawa CFTs and Emergent Supersymmetry. *PTEP*, 2016(12):12C105, 2016.
- [17] E. Grosfeld and A. Stern. Electronic transport in an array of quasiparticles in the $\nu=5/2$ non-Abelian quantum Hall state. , 73(20):201303, May 2006.
- [18] Y. Kamiya, A. Furusaki, J. C. Y. Teo, and G.-W. Chern. Majorana Stripe Order on the Surface of a Three-Dimensional Topological Insulator. *ArXiv e-prints*, November 2017.
- [19] C. Li and M. Franz. Majorana-Hubbard model on the honeycomb lattice. *ArXiv e-prints*, June 2018.
- [20] H. B. Nielsen and M. Ninomiya. Absence of neutrinos on a lattice. *Nucl. Phys. B*, 185:20, 1981.
- [21] Igor F. Herbut. Interactions and phase transitions on graphene’s honeycomb lattice. *Phys. Rev. Lett.*, 97:146401, Oct 2006.
- [22] Igor F. Herbut, Vladimir Juričić, and Bitan Roy. Theory of interacting electrons on the honeycomb lattice. *Phys. Rev. B*, 79:085116, Feb 2009.
- [23] Igor F. Herbut, Vladimir Juricic, and Oskar Vafek. Relativistic Mott criticality in graphene. *Phys. Rev.*, B80:075432, 2009.
- [24] T. Grover, D.N. Sheng, and A. Vishwanath. Emergent space-time supersymmetry at the boundary of a topological phase. *Science*, 344:280, 2014.

- [25] Michael E. Peskin and Daniel V. Schroeder. *An Introduction to quantum field theory*. Addison-Wesley, Reading, USA, 1995.
- [26] Alexander Altland and Ben Simons. *Condensed matter field theory; 2nd ed.* Cambridge Univ. Press, Cambridge, 2010.
- [27] Nikolai Zerf, Chien-Hung Lin, and Joseph Maciejko. Superconducting quantum criticality of topological surface states at three loops. *Phys. Rev.*, B94(20):205106, 2016.
- [28] Kenneth G. Wilson. The renormalization group: Critical phenomena and the kondo problem. *Rev. Mod. Phys.*, 47:773–840, Oct 1975.
- [29] Nikolai Zerf, Luminita N. Mihaila, Peter Marquard, Igor F. Herbut, and Michael M. Scherer. Four-loop critical exponents for the gross-neveu-yukawa models. *Phys. Rev. D*, 96:096010, Nov 2017.
- [30] Lorenzo Di Pietro and Emmanuel Stamou. Scaling dimensions in QED₃ from the ϵ -expansion. *JHEP*, 12:054, 2017.
- [31] Joshua Ellis. TikZ-Feynman: Feynman diagrams with TikZ. *Comput. Phys. Commun.*, 210:103–123, 2017.
- [32] Nathan Seiberg. Naturalness versus supersymmetric nonrenormalization theorems. *Phys. Lett.*, B318:469–475, 1993.
- [33] Marcus T. Grisaru, W. Siegel, and M. Rocek. Improved Methods for Supergraphs. *Nucl. Phys.*, B159:429, 1979.
- [34] Nikolay Bobev, Sheer El-Showk, Dalimil Mazáč, and Miguel F. Paulos. Bootstrapping the three dimensional supersymmetric ising model. *Phys. Rev. Lett.*, 115:051601, Jul 2015.
- [35] M. Oshikawa. Ordered phase and scaling in Z_n models and the three-state antiferromagnetic Potts model in three dimensions. *Phys. Rev. B*, 61:3430–3434, February 2000.
- [36] J. Manuel Carmona, A. Pelissetto, and E. Vicari. N-component Ginzburg-Landau Hamiltonian with cubic anisotropy: A six-loop study. *Phys. Rev. B*, 61:15136–15151, June 2000.
- [37] Jie Lou, Anders W. Sandvik, and Leon Balents. Emergence of $u(1)$ symmetry in the 3d xy model with Z_q anisotropy. *Phys. Rev. Lett.*, 99:207203, Nov 2007.

Appendix A

Derivation of the Low Energy Field Theory

In this appendix, we derive (2.11), which is the low energy continuum description of (2.3).

A.1 Quadratic Hamiltonian

Relabelling the Majorana operators γ according to (2.8), the first term of (2.3) becomes

$$H_0 = it \sum_{m,n} \gamma_{m,2n}^e [\gamma_{m+1,2n}^e + \gamma_{m,2n+1}^o] + \gamma_{m,2n+1}^o [-\gamma_{m+1,2n+1}^o + \gamma_{m,2n+2}^e]. \quad (\text{A.1})$$

Now using the expansion (2.10), the first piece of (A.1) is

$$\gamma_{m,2n}^e [\gamma_{m+1,2n}^e + \gamma_{m,2n+1}^o] \approx \quad (\text{A.2})$$

$$8\Lambda_0^{-2} [\chi^{e+}(m, 2n) + (-1)^m \chi^{e-}(m, 2n)] [\chi^{e+}(m+1, 2n) + (-1)^{m+1} \chi^{e-}(m+1, 2n) + \chi^{o+}(m, 2n+1) + (-1)^m \chi^{o-}(m, 2n+1)]$$

where we've suppressed the lattice constant a in the arguments of χ .

To derive a continuum field theory, we will Taylor expand the fields χ about the point $a(m + \frac{1}{2}, 2n + \frac{1}{2})$. Let $\chi := \chi(m + \frac{1}{2}, 2n + \frac{1}{2})$, and define

$$\partial_{\pm} := \frac{1}{2}(\partial_x \pm \partial_y). \quad (\text{A.3})$$

Each derivative will contribute an additional factor of lattice spacing $a = \Lambda_0^{-1}$. Then (A.2) becomes, after an integration by parts,

$$8\Lambda_0^{-2} \sum_{\pm} \pm \chi^{e\pm} e^{a\partial_x} \chi^{e\pm} + \chi^{e\pm} e^{a\partial_y} \chi^{o\pm} \quad (\text{A.4})$$

A.2. Quartic Hamiltonian

where we've dropped alternating terms that do not contribute to the low energy theory. Performing a similar expansion for the second piece of (A.1), and adding both contributions together yields

$$8\Lambda_0^{-2} \sum_{\pm} \pm \chi^{e\pm} e^{a\partial_x} \chi^{e\pm} \mp \chi^{o\pm} e^{a\partial_x} \chi^{o\pm} + \chi^{e\pm} [e^{a\partial_y} - e^{-a\partial_y}] \chi^{o\pm} \quad (\text{A.5})$$

Note that even-derivative functions vanish when sandwiched between the same Majorana operator, since integration by parts gives

$$\chi \partial^{(2k)} \chi = (-1)^{2k} \partial^{(2k)} \chi \chi, \quad (\text{A.6})$$

and $\{\chi, \partial^{(2k)} \chi\} = 0$. Therefore we can replace $e^{a\partial_x}$ by its odd part. Finally, using

$$\sum_{m,n} \mapsto \frac{1}{2} \Lambda_0^2 \int dx dy \quad (\text{A.7})$$

we find that the quadratic Hamiltonian density is

$$\mathcal{H}_0 + \mathcal{H}'_2 = 4it \sum_{\pm} \pm \chi^{e\pm} \sinh(a\partial_x) \chi^{e\pm} \mp \chi^{o\pm} \sinh(a\partial_x) \chi^{o\pm} + 2\chi^{e\pm} \sinh[a\partial_y] \chi^{o\pm} \quad (\text{A.8})$$

In Section 2.3, it is shown that the underlying symmetry of the lattice model forces all quadratic operators to preserve the emergent U(1) symmetry. Therefore, in our leading order study of U(1) breaking operators, we neglect the effects of \mathcal{H}'_2 .

A.2 Quartic Hamiltonian

We now repeat the steps of (A.1) for the interacting piece of (2.3), which splits into two pieces:

$$\mathcal{H}_{\text{int}} = g \sum_{m,n} \gamma_{m,2n}^e \gamma_{m+1,2n}^e \gamma_{m+1,2n+1}^o \gamma_{m,2n+1}^o + \gamma_{m,2n+1}^o \gamma_{m+1,2n+1}^o \gamma_{m+1,2n+2}^e \gamma_{m,2n+2}^e \quad (\text{A.9})$$

We are only required to Taylor expand the following object

$$A^{e/o}(x, y) := \gamma^{e/o}(x, y) \gamma^{e/o}(x + a, y) \quad (\text{A.10})$$

where $(x, y) = a(m + \frac{1}{2}, 2n + \frac{1}{2})$. In terms of this function, \mathcal{H}_{int} can be written as

$$\mathcal{H}_{\text{int}} = -\frac{g}{2} \Lambda_0^2 \left[A^e(x - a/2, y - a/2) A^o(x - a/2, y + a/2) \right] \quad (\text{A.11})$$

A.3. Leading $U(1)$ Breaking Operator

$$+A^e(x-a/2, y+a/2)A^o(x-a/2, y-a/2)\Big].$$

Using (A.11), and expanding up to two derivatives,

$$A(x-a/2, y-a/2) \approx 8\Lambda_0^{-2} \sum_{\pm} \pm [a\chi^{\pm}(\partial_+ + \partial_-)\chi^{\pm} - a^2\partial_+\chi^{\pm}\partial_-\chi^{\pm} + \frac{a^2}{2}(\partial_+^2 - \partial_-^2)\chi^{\pm}\chi^{\pm}]$$

(A.12)

$$+8\Lambda_0^{-2}(-1)^m \sum_{\pm} \pm [\chi^{\mp}\chi^{\pm} + a\chi^{\mp}(\partial_- - \partial_+)\chi^{\pm} - a^2\partial_+\chi^{\mp}\partial_-\chi^{\pm} + \frac{a^2}{2}\chi^{\mp}(\partial_-^2 + \partial_+^2)\chi^{\pm}]$$

where we've used the notation introduced in the previous subsection. Using this result, (A.7), and integration by parts, the Hamiltonian density can be written as

$$\frac{1}{64g\Lambda_0^{-4}}\mathcal{H}_{\text{int}} =$$

(A.13)

$$\begin{aligned} & - \sum_{s,s'=\pm 1} ss' \chi^{es} \partial_x \chi^{es} \chi^{os'} \partial_x \chi^{os'} - 4\Lambda_0^2 \chi^{e-} \chi^{e+} \chi^{o-} \chi^{o+} + 2\partial_y(\chi^{e-} \chi^{e+}) \partial_y(\chi^{o-} \chi^{o+}) \\ & + 2\chi^{e-} \chi^{e+} \partial_x \chi^{o-} \partial_x \chi^{o+} + 2\partial_x \chi^{e-} \partial_x \chi^{e+} \chi^{o-} \chi^{o+} + \partial_x(\chi^{e-} \chi^{e+}) \partial_x(\chi^{o-} \chi^{o+}) \end{aligned}$$

which is (2.12).

A.3 Leading $U(1)$ Breaking Operator

In this appendix, we derive (2.16), which is the $U(1)$ breaking piece of (A.13) in the ψ notation. For each type of term of (A.13), we insert the (inverses of) (2.15), and extract the $U(1)$ breaking part:

- Type 1:

$$\begin{aligned} & \chi^{e-} \chi^{e+} \partial_x \chi^{o-} \partial_x \chi^{o+} + \partial_x \chi^{e-} \partial_x \chi^{e+} \chi^{o-} \chi^{o+} \\ & = -\frac{1}{8}(\psi_2 \psi_1^* - \psi_2^* \psi_1)(\partial_x \psi_1 \partial_x \psi_2^* - \partial_x \psi_1^* \partial_x \psi_2) - \frac{1}{8}(\psi_2 \psi_1 - \psi_2^* \psi_1^*)(\partial_x \psi_1 \partial_x \psi_2 - \partial_x \psi_1^* \partial_x \psi_2^*) \\ & \rightarrow -\frac{1}{8}[\psi_2 \psi_1 \partial_x \psi_1 \partial_x \psi_2 + \text{h.c.}] \end{aligned}$$

(A.14)

- Type 2:

$$\begin{aligned} & \partial_i(\chi^{e-} \chi^{e+}) \partial_i(\chi^{o-} \chi^{o+}) \quad (\text{no sum over } i, \text{ and for } i = x, y) \\ & = -\frac{1}{4}(\partial_i \psi_2 \partial_i \psi_2^* \psi_1^* \psi_1 + \partial_i \psi_1^* \partial_i \psi_1 \psi_2 \psi_2^*) - \frac{1}{8}[\partial_i \psi_1 \partial_i \psi_2 + \partial_i \psi_1^* \partial_i \psi_2^*][\psi_1 \psi_2 + \psi_1^* \psi_2^*] \end{aligned}$$

A.3. Leading $U(1)$ Breaking Operator

$$\begin{aligned}
& -\frac{1}{8}[-\partial_i \psi_1 \psi_2^* - \partial_i \psi_1^* \psi_2][\psi_1^* \psi_2 + \psi_1 \psi_2^*] \\
& \rightarrow -\frac{1}{8}[\partial_i \psi_1 \partial_i \psi_2 \psi_1 \psi_2 + \text{h.c.}]
\end{aligned} \tag{A.15}$$

- Type 3:

$$\begin{aligned}
& (\chi^{e+} \partial_x \chi^{e+} - \chi^{e-} \partial_x \chi^{e-})(\chi^{o+} \partial_x \chi^{o+} - \chi^{o-} \partial_x \chi^{o-}) \\
& = -\frac{1}{4}(\partial_x \psi_1^* \partial_x \psi_1 \psi_1^* \psi_1 + \partial_x \psi_2 \partial_x \psi_2^* \psi_2 \psi_2^*) - \frac{1}{8}(\partial_x \psi_2 \partial_x \psi_1 + \partial_x \psi_2^* \partial_x \psi_1^*)(\psi_2 \psi_1 + \psi_2^* \psi_1^*) \\
& \quad - \frac{1}{8}(\partial_x \psi_2^* \partial_x \psi_1 + \partial_x \psi_2 \partial_x \psi_1^*)(\psi_2 \psi_1^* + \psi_2^* \psi_1) \\
& \rightarrow -\frac{1}{8}[\partial_x \psi_2 \partial_x \psi_1 \psi_2 \psi_1 + \text{h.c.}]
\end{aligned} \tag{A.16}$$

Using equations (A.14-A.16), we find that the $U(1)$ breaking piece of (A.13) is

$$16g_0\Lambda_0^4\psi_1\psi_2[\partial_x\psi_1\partial_x\psi_2 - \partial_y\psi_1\partial_y\psi_2] + \text{h.c.} \tag{A.17}$$

Since $\mathcal{H}_{\text{int}} = \mathcal{L}_{\text{int}}$ for an imaginary time Lagrangian density, we've reproduced (2.16).

Appendix B

Promoting ψ to a Dirac Fermion in Four Dimensions

One idea to resolve the issue of breaking Lorentz invariance in the ϵ -expansion is to promote ψ to a Dirac fermion in four dimensions. If this Dirac theory can be decoupled into two Weyl sectors, then we may obtain the Weyl renormalization group functions by continuing N , the number of Dirac fermions, from 1 to $\frac{1}{2}$ in this theory. We now show that this limit is ill-defined.

To generate the interaction term $\phi^* \psi^T C \psi$ in each Weyl sector, we consider following operator

$$i\phi^* \Psi^T \begin{pmatrix} C & 0 \\ 0 & -C \end{pmatrix} \Psi + \text{h.c.} \quad C = i\gamma^0 \quad (\text{B.1})$$

To show that it is Lorentz invariant, it is sufficient to consider $\psi^T C \psi$, since Lorentz transformations do not couple Weyl sectors in the Weyl basis. Using (3.33),

$$\psi^T C \psi \mapsto \psi^T e^{\vec{\alpha} \cdot \vec{\sigma}^T} C e^{\vec{\alpha} \cdot \vec{\sigma}} = \psi^T C e^{-\vec{\alpha} \cdot \vec{\sigma}} e^{\vec{\alpha} \cdot \vec{\sigma}} \psi = \psi^T C \psi \quad (\text{B.2})$$

under a general Lorentz transformation. Adding this interaction to the free Dirac Lagrangian density, we have

$$\mathcal{L} = \bar{\Psi} [\partial_a \Gamma^a + M] \Psi + [i\phi^* \Psi^T \begin{pmatrix} C & 0 \\ 0 & -C \end{pmatrix} \Psi + \text{h.c.}] \quad (\text{B.3})$$

By rotating $\psi_R \rightarrow \gamma_0 \psi_R$, so that both Weyl fermions propagate in the same direction, (B.3) becomes

$$\sum_{i=1}^2 [\bar{\psi}_i [\partial_\mu \gamma^\mu + i\partial_3] \psi_i + [i\phi^* \psi_i^T C \psi_i + \text{h.c.}]] + M \bar{\psi}_L \psi_R + \bar{\psi}_R \psi_L \quad (\text{B.4})$$

where we used (3.31). The two Weyl sectors can be decoupled by introducing

$$\psi_\pm := \frac{1}{\sqrt{2}} (\psi_L \pm \psi_R). \quad (\text{B.5})$$

Appendix B. Promoting ψ to a Dirac Fermion in Four Dimensions

This doesn't affect the interaction term, but it modifies the mass terms to

$$M[\bar{\psi}_L\psi_L - \bar{\psi}_R\psi_R] \tag{B.6}$$

This relative sign in the mass terms cannot be removed, implying that the two Weyl sectors are distinct. Any continuation of the Dirac number $N \rightarrow \frac{1}{2}$ would have to choose between one of these two distinct sectors, rendering the limit ill-defined.

Appendix C

Two Loop Calculation of the Fermion Mass Beta Function

In this appendix, we calculate β_M at the critical point $g_{c,2}$ in the massive theory, to two loop order in the modified ϵ -expansion. These calculations verify (5.33) to this order. While our one loop calculations were carried out in the Wilson picture of the renormalization group, it is easier to use dimensional regularization for higher order calculations. Following the conventions outlined in Section 3.3, we introduce counterterms, order-by-order, to cancel the divergences appearing in loop diagrams. Our task is to determine the renormalization constants that appear in the renormalized Lagrangian density

$$\mathcal{L} = Z_\psi \bar{\psi} [\not{\partial} + i\not{\partial}_3] \psi + M\mu Z_M \bar{\psi} \psi + Z_\phi |\partial_a \phi|^2 + \lambda_1 Z_{\lambda_1} \mu^{\epsilon/2} [\phi \psi^T C \psi + \text{h.c.}] + \lambda_2 Z_{\lambda_2} \mu^\epsilon |\phi^4| \quad (\text{C.1})$$

Here μ is an energy scale characterizing the RG flow; it plays a role analogous to b^{-1} in the Wilsonian picture. The factors of μ appearing in \mathcal{L} ensure the renormalized couplings and renormalized mass M are dimensionless. The beta function of M can be determined using the formulae

$$\beta_M = -[-1 - \gamma_\psi + \gamma_M] M \quad (\text{C.2})$$

$$\beta_X := -\frac{dX}{d\log \mu} \quad \gamma_X := -\frac{dZ_X}{d\log \mu} \quad (\text{C.3})$$

The negative signs present in the definitions of β_X and γ_X ensure that these functions have the same signs as their Wilsonian counterparts, $\frac{dX}{d\log b}$ and $\frac{dZ_X}{d\log b}$, where b is the length scale characterizing the size of a Wilsonian momentum shell. The anomalous dimensions satisfy

$$\gamma_x = \beta_{\lambda_1^2} \frac{d\log Z_x}{d\lambda_1^2} + \beta_{\lambda_2^2} \frac{d\log Z_x}{d\lambda_2^2} + \beta_M \frac{d\log Z_x}{dM} \quad (\text{C.4})$$

and provide a system of equations to find the beta functions at a given order. To determine the 2 loop anomalous dimensions, we require the 2

C.1. One Loop Diagrams

loop renormalization functions Z_M, Z_ψ , as well as the 1-loop beta functions $\beta_{\lambda_1^2}, \beta_M$, and $\beta_{\lambda_2^2}$.

In fact, it will turn out that Z_M and Z_ψ only depend on λ_1^2 to two loops, and so we only need to know $\beta_{\lambda_1^2}$. Because Z_M and Z_ψ are independent of M , we can use the massless one loop β function from [15]:

$$\beta_{\lambda_1^2} = -\epsilon\lambda_1^2 + \frac{3}{(4\pi)^2}\lambda_1^4 \quad (\text{C.5})$$

Once we verify that Z_ϕ, Z_ψ and Z_{λ_1} don't depend on M , it will be sufficient to calculate Z_ψ and Z_M to two loop order, to determine β_M .

In the following, all Feynman diagrams have been drawn using the package [31]. Solid lines correspond to fermion propagators, dashed lines correspond to boson propagators, and an arrow is used to indicate the direction of charge. This charge is +1 for the fermion propagator, and +2 for the boson propagator.

C.1 One Loop Diagrams

C.1.1 Fermion Propagator

At one loop, the fermion propagator is renormalized by a single diagram, shown in Figure C.1. It equals

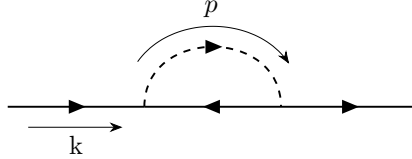


Figure C.1: Fermion self energy in renormalized perturbation theory

$$= (-2\lambda_1)^2 \int \frac{d^d p}{(2\pi)^d} D(p) C G^T(p-k) C = 4\lambda_1^2 \int \frac{d^d p}{(2\pi)^d} \frac{1}{p^2} \frac{i(\mathbf{p}^\dagger - \mathbf{k}^\dagger) - M}{(p-k)^2} \quad (\text{C.6})$$

where we've used

$$C(i\mathbf{p} + M)^T C = i\mathbf{p}^\dagger - M \quad (\text{C.7})$$

C.1. One Loop Diagrams

Introducing a Feynman parameter x according to

$$\frac{1}{p^2(p-k)^2} = \int_0^1 dx \frac{1}{[(p-xk)^2 + x(1-x)k^2]^2} \quad (\text{C.8})$$

and changing variables to $l = p - xk$, we have the diagram equalling

$$4\lambda_1^2 \int_0^1 dx \int \frac{d^d l}{(2\pi)^d} \frac{i(l^\dagger + (x-1)\mathbf{k}^\dagger) - M}{[l^2 + \Delta]^2} \quad (\text{C.9})$$

where

$$\Delta := x(1-x)k^2 \quad (\text{C.10})$$

Finally, using the integral formula

$$\int \frac{d^d l}{(2\pi)^d} \frac{1}{[l^2 + \Delta]^n} = \frac{1}{(4\pi)^{d/2}} \frac{\Gamma(n - \frac{d}{2})}{\Gamma(n)} \Delta^{\frac{d}{2}-n} \quad (\text{C.11})$$

we find that the diagram (C.1) equals

$$4\lambda_1^2 \int_0^1 dx [i(x-1)\mathbf{k}^\dagger - M] \frac{\Delta^{\frac{d}{2}-2}}{(4\pi)^{d/2}} \frac{\Gamma(2 - \frac{d}{2})}{\Gamma(2)} \quad (\text{C.12})$$

Replacing d with $4 - \epsilon$, we find that (C.1) has the following diverging term in the $\epsilon \rightarrow 0$ limit:

$$- \frac{4\lambda_1^2}{(4\pi)^2} \left[\frac{i}{2} \mathbf{k}^\dagger + M \right] \frac{2}{\epsilon} \quad (\text{C.13})$$

To cancel this divergence, we introduce renormalization constants δZ_ψ and δZ_M into the Lagrangian density, that produce the following terms to this order in λ_1^2 :

$$- i\delta Z_\psi \bar{\psi} \mathbf{k}^\dagger \psi + M\delta Z_M \bar{\psi} \psi \quad (\text{C.14})$$

Note that the renormalization constants in (C.1) satisfy

$$Z_x = 1 + \delta Z_x + \text{two loop terms} \quad (\text{C.15})$$

To achieve cancellation, we require

$$\delta Z_\psi = -\frac{4\lambda_1^2}{(4\pi)^2\epsilon} \quad \delta Z_M = \frac{8\lambda_1^2}{(4\pi)^2\epsilon} \quad (\text{C.16})$$

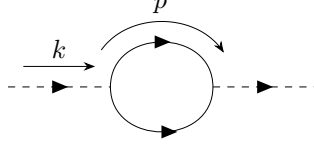


Figure C.2: Boson self energy in renormalized perturbation theory

C.1.2 Boson Propagator

At one loop, the boson propagator is renormalized by the single diagram in Figure C.2. It equals

$$= -\frac{1}{2}(-2\lambda_1^2) \int \frac{d^d p}{(2\pi)^d} \text{tr} CG(p) CG^T(k-p) \quad (\text{C.17})$$

The factor of $\frac{1}{2}$ is a symmetry factor, and the overall minus sign is determined from Wick's theorem, and is a common feature of fermion traces in Feynman diagrams. Introducing the same Feynman parameter as in (C.8), this equals

$$- \frac{4\lambda_1^2}{2} \int \frac{d^d p}{(2\pi)^d} \frac{d^d l p}{(2\pi)^d} \text{tr}[(i\mathbf{p} + M)(i\mathbf{k}^\dagger - i\mathbf{p}^\dagger - M)] \frac{1}{p^2(k-p)^2} \quad (\text{C.18})$$

$$= -\frac{4\lambda_1^2}{2} \int_0^1 dx \int \frac{d^d l}{(2\pi)^d} \frac{\text{tr}[l^2 - x(1-x)k^2 + iM(1-x)\mathbf{k}^\dagger - iMx\mathbf{k}]}{[l^2 + \Delta]^2} \quad (\text{C.19})$$

While $\text{tr} \not{p} = 0$

$$\text{tr} M \mathbf{p} = -2p_3 M \neq 0 \quad (\text{C.20})$$

However, this term is not Lorentz invariant, and can be dropped using the modified ϵ expansion introduced in the previous section. Using a secondary integral formula

$$\int \frac{d^d l}{(2\pi)^d} \frac{l^2}{[l^2 + \Delta]^n} = \frac{\Delta^{\frac{d}{2}+1-n}}{(4\pi)^{d/2}} \frac{d}{2} \frac{\Gamma(n - \frac{d}{2} - 1)}{\Gamma(n)} \quad (\text{C.21})$$

we find the one loop integral (C.2) equals

$$- \frac{4\lambda_1^2}{(4\pi)^{d/2}} \int_0^1 dx \left[\frac{d}{2} \Gamma(-1 + \frac{\epsilon}{2}) - \Gamma(\frac{\epsilon}{2}) \right] \Delta^{1-\frac{\epsilon}{2}} \quad (\text{C.22})$$

C.2. Two Loop Diagrams

Now using

$$\left[\frac{\epsilon}{2} - 1\right] \Gamma\left(\frac{\epsilon}{2} - 1\right) = \Gamma\left(\frac{\epsilon}{2}\right) \quad (\text{C.23})$$

and

$$\Gamma\left(\frac{\epsilon}{2} - 1\right) = -\frac{2}{\epsilon} + \mathcal{O}(1) \quad (\text{C.24})$$

the divergent behaviour as $\epsilon \rightarrow 0$ in (C.22) is

$$\frac{4\lambda_1^2}{(4\pi)^2} \int_0^1 dx \frac{6\Delta}{\epsilon} = \frac{\lambda_1^2}{(4\pi)^2} \frac{k^2}{\epsilon} \quad (\text{C.25})$$

To cancel this divergence, we introduce a counterterm δZ_ϕ that appears in the Lagrangian density as

$$k^2 \delta Z_\phi |\phi|^2 \quad (\text{C.26})$$

To achieve a cancellation, we require

$$\delta Z_\phi = -\frac{4\lambda_1^2}{(4\pi)^2 \epsilon} \quad (\text{C.27})$$

C.1.3 Interaction Vertex

At one loop there is no diagram renormalizing the fermion-boson interaction, so that $\delta Z_{\lambda_1} = 0$. Moreover, the diagrams renormalizing the pure boson interaction involve only the field ϕ at one loop order. Therefore, all renormalization constants are independent of mass, so that we can safely use the one loop result for $\beta_{\lambda_1^2}$, (C.5), from [15]. Now, we must find the two loop contributions to Z_ψ and Z_M .

C.2 Two Loop Diagrams

There are two types of diagrams contributing at two loops. Some are identical to (C.1), but with either the internal boson or internal fermion augmented with a one loop counterterm δZ_ϕ or δZ_ψ . We call these counterterm diagrams:

C.2.1 Boson Counterterm Diagram

The diagram involving an inserting of δZ_ϕ is shown in Figure C.3. It equals

$$= -\delta Z_\phi 4\lambda_1^2 \int \frac{d^d}{(2\pi)^d} D(p) C G^T(p-k) C \quad (\text{C.28})$$

C.2. Two Loop Diagrams

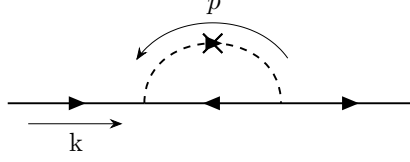


Figure C.3: Boson counterterm diagram in renormalized perturbation theory

We now wish to extract the diverging behaviour:

$$-\delta Z_\phi 4\lambda_1^2 \int \frac{d^d}{(2\pi)^d} D(p) C G^T(p-k) C \quad (C.29)$$

$$\begin{aligned} &\rightarrow -\delta Z_\phi 4\lambda_1^2 \int_0^1 dx [i(x-1)\not{\mathbf{k}}^\dagger - M] \frac{\Delta^{d/2-2}}{(4\pi)^{d/2}} \frac{\Gamma(2-\frac{d}{2})}{\Gamma(2)} \\ &= -\frac{4\lambda_1^2}{(4\pi)^2} \delta Z_\phi \int_0^1 dx [i(x-1)\not{\mathbf{k}}^\dagger - M] \left(\frac{\Delta}{(4\pi)^2} \right)^{-\frac{\epsilon}{2}} \left[\frac{2}{\epsilon} - \gamma + \mathcal{O}(\epsilon) \right] \quad (C.30) \end{aligned}$$

Now, in the \overline{MS} scheme (see Section 3.3), factors of γ and 4π are taken care of by rescaling the coupling constants appropriately. Therefore, the only diverging behaviour is

$$\frac{8}{\epsilon} \frac{\lambda_1^2}{(4\pi)^2} \delta Z_\phi \left[\frac{i}{2} \not{\mathbf{k}}^\dagger + M \right] \quad (C.31)$$

C.2.2 Fermion Counterterm Diagram

In the fermion counterterm diagram, displayed in Figure C.4, we replace the fermion propagator according to

$$\frac{1}{-i\not{\mathbf{p}} + M} \rightarrow \frac{1}{-i\not{\mathbf{p}} + M} (-i\delta Z_\psi \not{\mathbf{p}} - 2M\delta Z_\psi) \frac{1}{-i\not{\mathbf{p}} + M} \quad (C.32)$$

where we used $\delta Z_M = -2\delta Z_\psi$. This is

$$\frac{\delta Z_\psi}{-i\not{\mathbf{p}} + M} - 3M\delta Z_\psi \left(\frac{i\not{\mathbf{p}}}{p^2} \right)^2 \quad (C.33)$$

Replacing

$$(i\not{\mathbf{p}})^2 = -\not{\mathbf{p}}(\not{\mathbf{p}}^\dagger - 2ip_3) = -p^2 + 2i\not{\mathbf{p}}p_3 \rightarrow -p^2 \quad (C.34)$$

C.2. Two Loop Diagrams

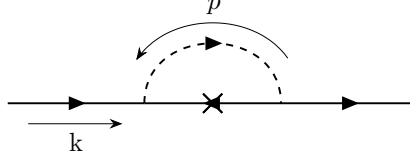


Figure C.4: Fermion counterterm diagram in renormalized perturbation theory

in the modified ϵ -expansion, we obtain

$$\frac{\delta Z_\psi}{-i\mathfrak{P} + M} + \frac{3M\delta Z_\psi}{p^2}. \quad (\text{C.35})$$

The diagram (C.4) then equals

$$-\delta Z_\psi 4\lambda_1^2 \int \frac{d^d p}{(2\pi)^d} D(p) \frac{i(\mathfrak{P}^\dagger - \mathbf{k}^\dagger) - 4M}{(p - k)^2} \quad (\text{C.36})$$

Using the calculations of (C.1), we find the following diverging behaviour:

$$\delta Z_\psi \frac{\lambda_1^2}{(4\pi)^2} \left[\frac{i}{2} \mathbf{k}^\dagger + 4M \right] \frac{8}{\epsilon} \quad (\text{C.37})$$

There are two remaining diagrams that contribute to β_M at two loops. One includes a fermion self energy bubble, and one includes a boson self energy bubble.

C.2.3 Internal Boson Bubble Diagram

The diagram including a boson self energy bubble is shown in Figure C.5. It equals

$$= -(-2\lambda_1)^2 \int \frac{d^d p}{(2\pi)^d} C G^T(p-k) C \frac{1}{p^4} \left[- \int_0^1 dx \frac{4\lambda_1^2}{(4\pi)^{d/2}} (3-\epsilon) [x(1-x)p^2]^{1-\frac{\epsilon}{2}} \Gamma(-1+\frac{\epsilon}{2}) \right] \quad (\text{C.38})$$

where we've used (C.22). Now, a generalized version of (C.8) lets us write

$$\frac{1}{(p-k)^2 [p^2]^{1+\frac{\epsilon}{2}}} = \int_0^1 dy \frac{(1-y)^{\epsilon/2}}{[l^2 + \Delta(y)]^{2+\frac{\epsilon}{2}}} \left[1 + \frac{\epsilon}{2} \right] \quad (\text{C.39})$$

C.2. Two Loop Diagrams

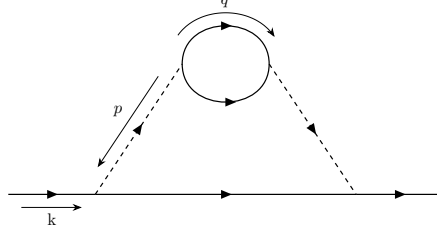


Figure C.5: Two loop diagram with internal boson bubble in renormalized perturbation theory

so that the diagram (C.5) equals

$$= -\frac{16\lambda_1^4}{(4\pi)^{d/2}} \left[1 + \frac{\epsilon}{2}\right]^2 (3-\epsilon)\Gamma\left(\frac{\epsilon}{2}\right) \int_0^1 dx dy [x(1-x)]^{1-\frac{\epsilon}{2}} \int \frac{d^d l}{(2\pi)^d} \frac{i(y-1)\mathbf{k}^\dagger - M}{[l^2 + \Delta(y)]^{2+\frac{\epsilon}{2}}} (1-y)^{\epsilon/2} \quad (\text{C.40})$$

$$= -\frac{16\lambda_1^4}{(4\pi)^d} \left[1 + \frac{\epsilon}{2}\right]^2 \frac{(3-\epsilon)\Gamma(\frac{\epsilon}{2})\Gamma(\epsilon)}{\Gamma(2+\frac{\epsilon}{2})} \int_0^1 dx dy [x(1-x)]^{1-\frac{\epsilon}{2}} (1-y)^{\epsilon/2} [i(y-1)\mathbf{k}^\dagger - M] \Delta^\epsilon \quad (\text{C.41})$$

where in the second line we used (C.11). The diverging behaviour is:

$$= -\frac{16\lambda_1^4}{(4\pi)^4} \left[1 + \frac{\epsilon}{2}\right]^2 \frac{(3-\epsilon)\Gamma(\frac{\epsilon}{2})\Gamma(\epsilon)}{(1+\frac{\epsilon}{2})^2 \Gamma(\frac{\epsilon}{2})} \int_0^1 dx dy [x(1-x)]^{1-\frac{\epsilon}{2}} (1-y)^{\epsilon/2} [i(y-1)\mathbf{k}^\dagger - M] \quad (\text{C.42})$$

Now, using the expansions

$$\int_0^1 dx [x(1-x)]^{1-\frac{\epsilon}{2}} = \frac{1}{6} + \frac{5\epsilon}{36} + \mathcal{O}(\epsilon^2) \quad (\text{C.43})$$

$$\int_0^1 dy (y-1)(1-y)^{\epsilon/2} = -\frac{1}{2} + \frac{\epsilon}{8} + \mathcal{O}(\epsilon^2) \quad (\text{C.44})$$

$$\int_0^1 dy (1-y)^{\epsilon/2} = 1 - \frac{\epsilon}{2} \quad (\text{C.45})$$

The expression (C.42) simplifies to

$$= -\frac{1}{\epsilon} \frac{16\lambda_1^4}{(4\pi)^4} [1 + \epsilon] \Gamma(\epsilon) \int_0^1 dy (1-y)^{\epsilon/2} [-i(y-1)\mathbf{k}^\dagger - M] \quad (\text{C.46})$$

$$= -\frac{1}{\epsilon} \frac{16\lambda_1^4}{(4\pi)^4} \Gamma(\epsilon) \left[-\frac{i}{2} \mathbf{k}^\dagger \left[1 + \frac{3\epsilon}{4}\right] - M \left[1 + \frac{\epsilon}{2}\right] \right] \quad (\text{C.47})$$

C.2. Two Loop Diagrams

Finally, \overline{MS} lets us replace $\Gamma(\epsilon) \rightarrow \frac{1}{\epsilon}$:

$$= \frac{1}{\epsilon^2} \frac{16\lambda_1^4}{(4\pi)^4} \left[\frac{i}{2} \mathbf{k}^\dagger \left[1 + \frac{3\epsilon}{4} \right] - M \left[1 + \frac{\epsilon}{2} \right] \right] \quad (\text{C.48})$$

We record this result and move to the final diagram.

C.2.4 Internal Fermion Bubble Diagram

The final diagram is shown in Figure C.6. It equals

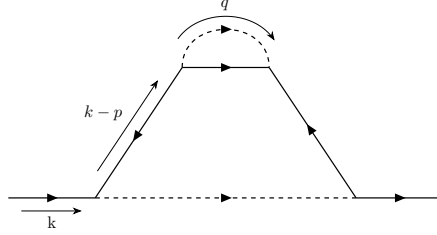


Figure C.6: Two loop diagram with internal fermion bubble in renormalized perturbation theory

$$= -4\lambda_1^2 \int \frac{d^d p}{(2\pi)^d} D(p) C G^T(p-k) \Sigma_\psi(p-k)^T G^T(p-k) C \quad (\text{C.49})$$

where Σ_ψ is the one loop fermion self energy diagram (C.1). The integrand is

$$\begin{aligned} & D(p) C G^T(p-k) C^2 \Sigma(p-k)^T C^2 G^T(p-k) C \\ &= \frac{4\lambda_1^2 \Gamma(\frac{\epsilon}{2})}{(4\pi)^{d/2}} \int_0^1 dx C G^T(p-k) C [i(x-1)(\mathbf{p}-\mathbf{k}) + M] C G^T(p-k) C \Delta^{-\frac{\epsilon}{2}} \end{aligned} \quad (\text{C.50})$$

(where we used $C \mathbf{p}^{\dagger T} C = \mathbf{p}$). We can rearrange the propagator factors according to

$$C G^T(p) C [i(x-1)\mathbf{p} + M] C G^T(p) C \quad (\text{C.52})$$

$$= \frac{1}{-i\mathbf{p} - M} [i(x-1)\mathbf{p} + M] \frac{1}{-i\mathbf{p} - M} = \frac{(x-1)[i\mathbf{p} + M]}{-i\mathbf{p} - M} + \frac{(2-x)M}{(-i\mathbf{p} - M)^2} \quad (\text{C.53})$$

$$= \frac{i(1-x)\mathbf{p}^\dagger - (3-2x)M}{p^2} + \mathcal{O}(M^2) \quad (\text{C.54})$$

C.2. Two Loop Diagrams

where in the last line we made the replacement (C.34). The diagram (C.6) then equals

$$-\frac{16\lambda_1^4\Gamma(\frac{\epsilon}{2})}{(4\pi)^{d/2}} \int_0^1 dx [x(1-x)]^{-\epsilon/2} \int \frac{d^d p}{(2\pi)^d} \frac{1}{p^2} \left[\frac{i(1-x)(\mathbf{p}^\dagger - \mathbf{k}^\dagger) - (3-2x)M}{(p-k)^{2+\epsilon}} \right] \quad (\text{C.55})$$

Introducing a Feynman parameter as in (C.39),

$$\frac{1}{(p-k)^{2+\epsilon} p^2} = \int_0^1 dy \frac{y^{\epsilon/2}}{[l^2 + \Delta(y)]^{2+\frac{\epsilon}{2}}} \left[1 + \frac{\epsilon}{2} \right] \quad (\text{C.56})$$

we have

$$\begin{aligned} & - \left[1 + \frac{\epsilon}{2} \right] \frac{16\lambda_1^4\Gamma(\frac{\epsilon}{2})}{(4\pi)^{d/2}} \int_0^1 dy dx [x(1-x)]^{-\epsilon/2} y^{\epsilon/2} \\ & \times \int \frac{d^d l}{(2\pi)^d} \frac{1}{[l^2 + \Delta(y)]^{2+\frac{\epsilon}{2}}} \left[i(1-x)(y-1)\mathbf{k}^\dagger - (3-2x)M \right] \\ & = -\frac{2}{\epsilon} \Gamma(\epsilon) \frac{16\lambda_1^4}{(4\pi)^d} \int_0^1 dy dx [x(1-x)]^{-\epsilon/2} y^{\epsilon/2} \left[i(1-x)(y-1)\mathbf{k}^\dagger - (3-2x)M \right] \Delta^{-\epsilon} \end{aligned} \quad (\text{C.57})$$

where in the last line we used (C.11). In the \overline{MS} scheme, we replace $\Gamma(\epsilon) \rightarrow \frac{1}{\epsilon}$. Therefore, the divergent piece of (C.6) is

$$= -\frac{2}{\epsilon^2} \frac{\lambda_1^4}{(4\pi)^d} \int_0^1 dy dx [x(1-x)]^{-\epsilon/2} y^{\epsilon/2} \left[i(1-x)(y-1)\mathbf{k}^\dagger - (3-2x)M \right] \quad (\text{C.58})$$

We now use the following expansions:

$$\int_0^1 dx x^{-\epsilon/2} (1-x)^{1-\epsilon/2} = \frac{\Gamma(1-\frac{\epsilon}{2})\Gamma(2-\frac{\epsilon}{2})}{\Gamma(3-\epsilon)} = \frac{1}{2}[1+\epsilon] + \mathcal{O}(\epsilon^2) \quad (\text{C.59})$$

$$\int_0^1 dx [x(1-x)]^{-\epsilon/2} = 1 + \epsilon + \mathcal{O}(\epsilon^2) \quad (\text{C.60})$$

$$\int_0^1 dy y^{\epsilon/2} = 1 - \frac{\epsilon}{2} + \mathcal{O}(\epsilon^2) \quad (\text{C.61})$$

$$\int_0^1 dy y^{\epsilon/2+1} = \frac{1}{2} - \frac{\epsilon}{8} + \mathcal{O}(\epsilon^2) \quad (\text{C.62})$$

We find the following divergent behaviour:

$$i\mathbf{k} \frac{16\lambda_1^4}{(4\pi)^4} \left[\frac{1}{2\epsilon^2} \left(1 + \frac{1}{4}\epsilon \right) \right] + M \frac{16\lambda_1^4}{(4\pi)^4} \frac{4}{\epsilon^2} \left(1 + \frac{\epsilon}{2} \right) \quad (\text{C.63})$$

C.2.5 Fermion Mass Beta Function

Adding up the divergences (C.31, C.37, C.48, C.64), we find

$$= \frac{8}{\epsilon} \frac{\lambda_1^2}{(4\pi)^2} \delta Z_\psi(i\mathbf{k}) + \frac{40}{\epsilon} \delta Z_\psi \frac{\lambda_1^2}{(4\pi)^2} M + (i\mathbf{k}) \frac{16\lambda_1^4}{(4\pi)^4} \left[\frac{1}{\epsilon^2} + \frac{1}{2\epsilon} \right] + M \frac{16\lambda_1^4}{(4\pi)^4} [5 + \epsilon] \quad (\text{C.65})$$

Using the one loop result

$$\delta Z_\psi = \frac{-4\lambda_1^2}{(4\pi)^2 \epsilon} \quad (\text{C.66})$$

the total divergence at two loops is

$$= -\frac{16\lambda_1^4}{(4\pi)^4} (i\mathbf{k}) \left[\frac{1}{\epsilon^2} - \frac{1}{2\epsilon} \right] - \frac{16\lambda_1^4}{(4\pi)^4} M \left[\frac{5}{\epsilon^2} - \frac{5}{2\epsilon} \right] \quad (\text{C.67})$$

This determines the renormalization constants to this order:

$$Z_\psi = 1 - \frac{4\lambda_1^2}{(4\pi)^2} - \frac{16\lambda_1^4}{(4\pi)^4 \epsilon^2} + \frac{8\lambda_1^4}{(4\pi)^4 \epsilon} \quad (\text{C.68})$$

$$Z_M = 1 + \frac{8\lambda_1^2}{(4\pi)^2 \epsilon} + \frac{80\lambda_1^4}{(4\pi)^4 \epsilon^2} - \frac{40\lambda_1^4}{(4\pi)^4 \epsilon} \quad (\text{C.69})$$

Having obtained Z_ψ and Z_M , we can now calculate their respective anomalous dimensions. Expanding:

$$\log Z_\psi = -\frac{4\lambda_1^2}{(4\pi)^2 \epsilon} - \frac{24\lambda_1^4}{(4\pi)^4 \epsilon^2} + \frac{8\lambda_1^4}{(4\pi)^4 \epsilon} + \mathcal{O}(\lambda_1^6) \quad (\text{C.70})$$

$$\log Z_M = \frac{8\lambda_1^2}{(4\pi)^2 \epsilon} + \frac{48\lambda_1^4}{(4\pi)^4 \epsilon^2} - \frac{40\lambda_1^4}{(4\pi)^4 \epsilon} + \mathcal{O}(\lambda_1^6) \quad (\text{C.71})$$

Then differentiating and using the one loop beta function (C.5), we find

$$\gamma_\psi = \beta_{\lambda_1^2} \frac{d \log Z_\psi}{d \lambda_1^2} = -\frac{4\lambda_1^2}{(4\pi)^2} + \frac{16\lambda_1^4}{(4\pi)^4} \quad (\text{C.72})$$

and

$$\gamma_M = \frac{8\lambda_1^2}{(4\pi)^2} - \frac{80\lambda_1^4}{(4\pi)^4} \quad (\text{C.73})$$

Therefore, the beta function is

$$\beta_M = M [1 + \gamma_\psi - \gamma_M] = M - \frac{12\lambda_1^2 M}{(4\pi)^2} + \frac{96\lambda_1^4 M}{(4\pi)^4} \quad (\text{C.74})$$

C.2. Two Loop Diagrams

Using the critical value of λ_1^2 found in [15],

$$\frac{\lambda_{1,*}^2}{(4\pi)^2} = \frac{\epsilon}{12} + \frac{\epsilon^2}{36} \quad (\text{C.75})$$

the beta function equals

$$\beta_M(\lambda_{1,*}) = \left[1 - 12 \left[\frac{\epsilon}{12} + \frac{\epsilon^2}{36} \right] + 96 \frac{\epsilon^2}{144} \right] M = \left[1 - \epsilon + \frac{\epsilon^2}{3} \right] M \quad (\text{C.76})$$

which agrees with the relation (5.33) to $\mathcal{O}(\epsilon^2)$.